

1 **Revisiting Panda 100, the first archaeological chimpanzee**
2 **nut-cracking site**

3
4 Proffitt. T.^{1*}, Haslam. M.², Mercader. J.F.³, Boesch. C.⁴, Luncz. L.V.⁵

5
6 ¹ Institute of Archaeology, University College London, 31-34 Gordon Square, London, WC1H 0PY

7 ² Primate Archaeology Research Group, School of Archaeology, University of Oxford, Dyson Perrins
8 Building, South Parks Road, Oxford OX1 3QY, United Kingdom

9 ³ Department of Anthropology and Archaeology, University of Calgary, 2500 University Dr., NW
10 Calgary, Alberta T2N 1N4, Canada

11 ⁴ Department of Primatology, Max Plank Institute for Evolutionary Anthropology, Deutscher Platz 6,
12 D - 04103 Leipzig, Germany

13 ⁵ School of Anthropology and Museum Ethnography, University of Oxford, Oxford, OX2 6PE, UK.

14
15 * Corresponding Author: t.proffitt@ucl.ac.uk

27 **Abstract**

28 Archaeological recovery of chimpanzee *Panda oleosa* nut cracking tools at the Panda 100 (P100) and
29 Noulo sites in the Taï Forest, Ivory Coast, showed that this behaviour is over 4,000 years old, making
30 it the oldest known evidence of non-human tool use. In 2002, the first report on P100 directly compared
31 its lithic assemblage to early hominin stone tools, highlighting their similarities and proposing the name
32 ‘Pandan’ for the chimpanzee material. Here we present an expanded and comprehensive technological,
33 microscopic, and refit analysis of the lithic assemblage from P100. Our re-analysis provides new data
34 and perspectives on the applicability of chimpanzee nut cracking tools to our understanding of the
35 percussive behaviours of early hominins. We identify several new refit sets, including the longest
36 hammerstone transport seen in the chimpanzee archaeological record. We provide detailed evidence of
37 the fragmentation sequences of *Panda* nut hammerstones, and characterise the percussive damage on
38 fragmented material from P100. Finally, we emphasise that the chimpanzee lithic archaeological record
39 is dynamic, with the preservation of actual hammerstones being rare, and the preservation of small
40 broken pieces more common. P100 - the first archaeological chimpanzee nut cracking lithic assemblage
41 - provides a valuable comparative sample by which to identify past chimpanzee behaviour elsewhere,
42 as well as similar hominin percussive behaviour in the Early Stone Age.

43

44 **Keywords:** Primate Archaeology; Panda 100; Lithic Analysis; West African Chimpanzee; Primate
45 Tool Use; Percussive Technology; Refit; *Pan troglodytes verus*

46

47

48 1. Introduction

49

50 Discussions of the evolution of tool use have historically centred on the hominin lineage: *Homo sapiens*
51 and our ancestors since we split from the other apes (Harmand et al., 2015; Leakey, 1971). Hominin
52 technological evolution is recorded in a durable record of stone tools, which provide detailed
53 information about our cultural and cognitive development, extending back more than 3.3 million years
54 (Harmand et al., 2015). In contrast, our understanding of the technological evolution of non-human
55 primates is in its infancy. The emerging field of primate archaeology addresses this imbalance using
56 modern archaeological techniques to understand the emergence and development of primate tool use,
57 and to provide new comparative insights into the emergence of hominin lithic technology (Haslam,
58 2012, Haslam et al, 2017).

59 Owing to their close relatedness to humans, and their propensity to use a variety of tools, chimpanzees
60 received the earliest and most intense attention as a potential model species for understanding early
61 hominin stone tool use. Some West African chimpanzees (*Pan troglodytes verus*) use stone tools in the
62 wild, primarily to crack open different nut species. Two long term study sites - Bossou in Guinea and
63 the Taï National Park in Côte d'Ivoire - provide the majority of the research data on this behaviour. In
64 the Taï National Park chimpanzees crack open five different nut species (*Panda oleosa*, *Parinari*
65 *excelsa*, *Saccoglottis gabonensis*, *Coula edulis*, and *Detarium senegalensis*). To crack open the very
66 hard *P. oleosa* nuts chimpanzees use stone tools that vary in size between 3 and 15 kg (Boesch and
67 Boesch, 1984a), and mostly tree roots for anvils. The uneven distribution of stone material throughout
68 the forest means that chimpanzees need to transport hammerstones to supply *Panda* nut trees with
69 suitable tool material (Boesch and Boesch, 1984a; Luncz et al., 2016).

70 In 2002, Mercader et al. published a pioneering study from the Taï Forest, proving that inactive
71 chimpanzee stone tool behavioural sites are identifiable in the archaeological record. For the first time
72 researchers demonstrated that a primate material record existed and could be traced, using
73 archaeological techniques, into antiquity. In addition, Mercader et al. (2002) suggested that the
74 chimpanzee artefactual record uncovered at their research site Panda 100 (P100) mimicked early
75 hominin lithic technology. Specific attention was paid to its apparent similarities to Early Stone Age
76 (ESA) lithic assemblages from Omo 123 (Chavaillon, 1976, 1970; de la Torre, 2004), the Shungura
77 formation (FtJi1) (Merrick et al., 1973; Merrick and Merrick, 1976) and KBS Member (Koobi Fora,
78 Kenya) (Isaac, 1976). This led to the suggestion that some lithic material from such Oldowan
79 assemblages may derive from nut cracking behaviour, or the processing of other hard-object foods. This
80 finding contributed directly to the emergence of primate archaeology as a new discipline, combining
81 both archaeological techniques and primate behavioural observations (Haslam et al., 2016a, 2016b,

82 2009, 2017). Here, we apply the latest primate archaeological methods to the P100 lithic assemblage,
83 providing new insights into the relevance of this material for interpreting hominin behaviour (Haslam,
84 2012).

85

86 2. Background

87

88 The P100 site was a known modern chimpanzee nut cracking location. The 100 square meter excavation
89 at the site yielded a substantial artefactual record, including both lithics and organic remains in the form
90 of abundant nut shells and wooden anvils. This study was joined by subsequent excavations at Noulo
91 and Sacoglotis B, dated to over 4,000 years ago, and located within a hundred metres of P100 (Mercader
92 et al., 2007). The stones recovered from P100 were proposed as the ‘Pandan’ type assemblage, that is,
93 the type assemblage against which future chimpanzee archaeological finds could be assessed (Mercader
94 et al., 2002).

95 Although not explicitly stating that hominin-like conchoidal flake technology was represented at P100,
96 Mercader et al. identified numerous pieces that they classified as ‘flakes’ within the assemblage, noting
97 that ‘panins may have been capable of producing assemblages that mimic some of the earliest hominin
98 artifacts’ (Mercader et al., 2002, p1455). The apparent similarity of the P100 lithic assemblage to
99 Oldowan hominin stone tool technology has been discussed and contested by a number of researchers
100 (de la Torre, 2004; Delagnes and Roche, 2005; Harmand et al., 2015; Pelegrin, 2005; Schick and Toth,
101 2006).

102 Since the initial publication of the P100 material, the study of non-flaking percussive technology has
103 taken a far more prominent and important role in the study of early hominin lithic technology and human
104 evolution. For example, re-analysis of the Omo Oldowan lithic assemblages have argued for the
105 presence of relatively structured exploitation strategies there, including the structured production of
106 fully conchoidal flakes (de la Torre, 2004). Both the quality and diminutive dimensions of the available
107 raw material at Omo are a major factor in the apparently simple nature of the assemblages, and de la
108 Torre et al. (2004) found that any similarity to the P100 lithic material was only in terms of dimensions.
109 The lithic material produced by early hominins appeared qualitatively different to that identified at
110 P100, and indeed to captive primate knapped artefacts (Delagnes and Roche, 2005; Pelegrin, 2005;
111 Schick and Toth, 2006). The importance of percussive activities involving both an active hammerstone
112 and a passive anvil have also recently been highlighted in the human archaeological record at Olduvai
113 (de la Torre et al., 2013; Mora and de la Torre, 2005), West Turkana (Harmand et al., 2015; Lewis and
114 Harmand, 2016), and Gesher Benot Yaqov (Goren-Inbar et al., 2015, 2002).

115 Research into percussive technology has focused on the Plio-Pleistocene archaeological record,
116 particularly in East Africa, where percussive behaviours played an important role in the subsistence
117 strategies of early hominins (de la Torre and Mora, 2005; Mora and de la Torre, 2005). To identify this
118 type of behaviour, a number of studies have developed referential data sets that characterize the
119 archaeological signature of percussive activities (Arroyo, 2015; Caruana et al., 2014; de la Torre et al.,
120 2013). These studies have either experimentally replicated percussion on the same raw materials
121 identified in the archaeological record (Arroyo, 2015; de la Torre et al., 2013), or quantified the wear
122 patterns associated with intentional percussive activities verses natural taphonomic damage (Caruana
123 et al., 2014). For example, de la Torre et al. (2013) found that experimental activities such as nut
124 cracking, bipolar knapping, meat tenderizing and plant processing produced a range of use-damage on
125 the passive hammer (anvil) involved in the behaviour. This damage included archaeologically
126 identifiable detached pieces, corresponding with typical percussive anvil products identified in the
127 archaeological record (De la Torre and Mora, 2005). More recently, the importance of primate
128 percussive technology and behaviours for interpreting the hominin archaeological record has been
129 highlighted using GIS analytical techniques on tools used in field experiments (Benito-Calvo et al,
130 2015) and by captive chimpanzees (Arroyo et al., 2016).

131 Beyond chimpanzees, recent research with other tool-using primates provides insights into the
132 emergence of hominin flake technology. For example, wild bearded capuchin monkeys in Serra da
133 Capivara National Park (SCNP), Brazil, intentionally strike quartz cobbles together, unintentionally
134 producing numerous fully conchoidal flakes (Proffitt et al., 2016). These flakes, resulting from the only
135 recorded behaviour where wild primates deliberately strike stone tools on other stones, exhibit the same
136 range of technological attributes commonly identified in hominin flaked assemblages. The
137 identification of such artefacts in the primate record has relevance to the suggestion that hominin flaked
138 technology may have initially emerged as a by-product of percussive behaviour (McGrew, 1992). This
139 combination of new information regarding the technology of hominin percussive material in the East
140 African archaeological record, and the identification of truly flaked primate (capuchin) artefacts,
141 reaffirms the importance of the P100 lithic assemblage as a potentially valuable comparative dataset for
142 the characterisation and identification of percussive behaviour in the archaeological record.

143 Here, we present a complete technological analysis of the lithic material excavated from the P100 site.
144 The combined technological, refit and microscopic analysis of this percussive material provides a finer
145 grained characterisation of the archaeological signature of wild chimpanzee nut cracking behaviour than
146 previously achieved. By renewing the analysis of the Panda 100 lithic material, this valuable
147 primatological assemblage can be of further use to researchers in understanding the emergence of both
148 West African chimpanzee and hominin percussive behaviour.

149

150 **3. Materials and methods**

151

152 3.1 *The Panda 100 site*

153 The P100 site is located within the Tai Forest in the western region of the Ivory Coast (**Figure 1A**) and
154 lies between the confluence of two rainforest streams that frequently inundate the surrounding area.
155 Mercader et al (2002) addressed the degree of spatial and artefactual integrity of the lithic assemblage,
156 noting that all material was identified in low energy sedimentary contexts, consisting of non-stratified
157 clay, silt and sand sediments. Coupled with the presence of numerous nut shells and a high frequency
158 of artefacts <20 mm (n=374 of 479 pieces; 78%) in maximum dimension, these data suggest that post-
159 depositional fluvial transportation of the assemblage was not a significant factor (Mercader et al., 2002).
160 In addition, the vast majority of the lithic artefacts possess fresh fractured edges, with very little
161 rounding of fractured surfaces, suggesting minimal fluvial effects.

162 P100 is in the immediate vicinity of a single *Panda* tree where chimpanzees were directly observed to
163 crack nuts with stone tools. During the occupation of this site, from at least 1975, stone hammers were
164 used in conjunction with wooden anvils, consisting of protruding tree roots. The site was eventually
165 abandoned in 1996 (Boesch and Boesch, 1984a; Mercader et al., 2002) when the *Panda* tree died and
166 fell to the ground. The immediate area is devoid of adequate raw material sources for use as
167 hammerstones, suggesting that all tools were actively carried to the vicinity of the *Panda* tree.

168 Archaeological excavation at P100 covered 59 m², excavated in arbitrary spits of 3 cm, concentrating
169 on the regions immediately surrounding four visible anvils. In addition, an excavation of the wider area
170 was conducted to a depth of 5 cm, resulting in the identification of two addition anvils. Fragmented
171 lithic material was associated with all anvil areas and a total of 479 artefacts were recorded, consisting
172 of four raw materials: granitoid, laterite, diorite, and quartzite. These were classified based on general
173 morphology into hammer edges, cortical and non-cortical flakes, tabular products, angular shatter,
174 amorphous shatter and microshatter (<20 mm) (Mercader et al., 2002). Of these artefact categories,
175 Mercader et al. paid particular attention to the flakes, arguing that these shared similar dimensional,
176 morphological and technological attributes to Oldowan flakes (Omo, Gona and Koobi Fora). They
177 identified partially and non-cortical flakes, and a single example with a dihedral striking platform
178 (Mercader et al., 2002). Seven refits (16 pieces) were also identified at two anvils, representing a
179 maximum horizontal movement of stone pieces of between 0.05 and 1.60 m.

180

181 **Insert Figure 1**

182 **Figure 1.** (A) Location map of Panda 100 (P100) site. (B) Updated excavation and refit map of P100
183 lithic assemblage (adapted from Mercader et al (2002) and updated with new digitised data from the
184 current study)

185 There are currently five published radiocarbon dates for the Panda 100 site (Mercader et al., 2007)
186 (**Table 1**). These dates were obtained from excavations in 2003, which extended the P100 excavations
187 into deeper and older sediments than those that contained the tools discussed in the present study. The
188 deeper sediments returned uncalibrated radiocarbon ages of 2330-4280 BP, which equate to 2182-4966
189 years BP when calibrated. These dates therefore do not reflect the age of the P100 artefacts reported in
190 2002 (Mercader et al., 2002) and re-analysed here. Instead, the lithic data presented here come from
191 artefacts most likely deposited in the second half of the twentieth century, including during the time of
192 observed use of the P100 sites by wild chimpanzees from 1979 to 1996.

193

194 **Table 1.** Uncalibrated and calibrated radiocarbon ages from the Panda 100 site (Mercader et al.,
195 2007), calibrated using OxCal 4.2 and the IntCal13 curve

Sample ^a	$\delta^{13}\text{C}$ %	¹⁴ C age BP	Years BP (68.2%) ^b	Years BP (95.4%) ^b
Beta-172916	-27.6	2330±40	2420-2311	2485-2182
Beta-164876	-27.9	2440±40	2684-2364	2705-2721
Beta-164877	-27.2	2440±40	2684-2364	2705-2721
Beta-172913	-26.8	3750±40	4218-3999	4235-3984
Beta-164879	-25	4280±40	4871-4827	4966-4711

196 ^a Sample depths below the site surface are not provided in the original publication

197 ^b 68.2% and 95.4% probability intervals

198

199 **3.2 Technological analysis**

200 For this study, all P100 lithic material was measured and weighed, with pieces >20 mm subjected to a
201 full technological analysis. In the original report of the P100 lithic material (Mercader et al., 2002) a
202 brief analysis of the lithic material included typological classifications and dimensions of the artefacts
203 as well as the range of raw materials present. Since that time a number of technological analyses have
204 been conducted on both hominin and primate percussive lithic assemblages. Of these de la Torre and
205 Mora (2005, 2013) have outlined a comprehensive techno-typological classificatory scheme for the
206 analysis of hominin lithic material derived from percussive behaviour. This classification system was

207 developed through the analysis of hominin passive anvils and their associated detached products, and
208 the analysis presented here draws on these classification schemes in order to characterise the P100 lithic
209 material. Mora and de la Torre (2005) set out five separate passive element percussive groups, based
210 on both the morphological location from which a fragment is derived and its technological
211 characteristics. These include edge products (Group 1.1), corner products (Group 1.2), elongated
212 detached pieces from the anvil faces (Group 2.1), angular chunks (Group 2.2), and detached pieces that
213 may resemble knapped flakes with a high degree of percussive damage (Group 2.3). Subsequently,
214 Arroyo (Arroyo, 2015; Arroyo and de la Torre, 2016) expanded on this classificatory system, to include
215 typical hammerstone flakes (Group 3), resembling knapping hammerstone unintentional detachments
216 which possess a convex ventral surface with no clear impact point, and angular fragments detached
217 spontaneously from an inactive region of the hammer or anvil (Group 4). In addition to these
218 classifications, artefacts smaller than 20 mm in maximum dimensions that exhibited no clear percussive
219 damage were classified as small debris (Group 5).

220

221 3.3 *Refit analysis*

222 A total of 471 artefacts underwent 40 hours of refitting. All artefacts were subjected to refit analysis,
223 using a raw material grouping as well as coordinate grouping. Initially artefacts from each anvil were
224 grouped followed by the grouping of all artefacts of each raw material. The vertical distance between
225 refits may reflect a degree of time depth. As precise coordinates for each artefact are not available, the
226 only way to assess vertical refit distance is through the variation in spits for each refit. Mercader et al.
227 (2002) report that each spit was arbitrarily defined as 3 cm thick, with a total of six spits being excavated
228 as well as material collected from the sub-surface.

229 An original refit study by Mercader et al. (2002) documented movement of artefacts at P100 over a
230 distance of 0.05-1.6 m. To determine horizontal distance between refits, the original excavation hand
231 drawn artefact maps were digitised using ArcMap and georeferenced to an internally coherent
232 coordinate system. In most cases refitted pieces were correlated to drawn artefacts in the original notes,
233 however, in a few cases (n=5) either no artefacts or a single artefact in the refit set could not be identified
234 in the original notes. To determine distance between refitted pieces, where possible, exact
235 measurements were taken using ArcMap, however, where no correlation with hand drawn notes was
236 possible distance was calculated by taking the measurements from the centre of associated grid
237 references (we have distinguished between these two methods of measurement in Table 4). It is
238 important to note that the distances reported in this study must be considered as minimum transportation
239 distances, as hammerstone movement by chimpanzees is well documented by direct observation, and
240 may consist of numerous individual transport events (Boesch and Boesch, 1984a; Luncz et al., 2016).

241 In addition to horizontal measurements, the vertical distance between refitted pieces was calculated
242 from spit designations.

243

244 3.4 *Microscopic analysis*

245 All lithic artefacts >20 mm in maximum dimension were macroscopically screened for evidence of
246 percussive damage. Potentially damaged areas were analysed using a low-powered magnification
247 (<100x) using a Leica S9APO stereo microscope equipped with a 1-8x objective lenses and a 10x
248 eyepiece. Microscopic photographs were taken using a 3.1Mp EC3 digital microscope camera.
249 Characterisation of use-wear damage followed the criteria of Adams et al. (Adams et al., 2006), which
250 has been successfully applied to other primate battered lithics (Arroyo, 2015; Arroyo and de la Torre,
251 2016).

252 4. **Results**

253

254 4.1 *Technological analysis*

255 4.1.1 General frequencies

256 The available lithic assemblage from Panda 100 consists of 473 artefacts, from five raw materials
257 including granitoid (n=376, 76.5%), laterite (n=80, 17.1%), diorite (n=9, 1.7%), quartzite (n=6, 1.3%)
258 and weathered clast (n=2, 0.4%). The two pieces of weathered clast have been omitted from the
259 following technological analysis as they are not mentioned in the original P100 report, may have entered
260 the archaeological record through natural processes, and are not likely to have been utilised by
261 chimpanzees as nut cracking hammerstones. In addition to this, all feldspar artefacts (originally reported
262 as coming solely from Anvil 4), a single quartzite and a single diorite piece reported by Mercader et al.
263 (2002) were not identified in this study, resulting in a mis-match of eight artefacts (1.67%).

264 The majority of the lithic assemblage is small debris (n=364, 77.3%), angular chunks (n=34, 7.2 %)
265 and angular fragments (n=25, 5.3%). Techno-typological categories more frequently associated with
266 percussive behaviour in the archaeological record are represented in low frequencies, such as corner
267 fragments (n=30, 6.4%), edge fragments (n=14, 3%), and typical hammerstone flakes (n=3, 0.6%).
268 Only one piece (0.2%) in the assemblage possesses a morphological similarity to detached flakes
269 (Table 2) (Supplementary Material 1).

270

271

272 **Table 2.** Absolute and relative frequency of technological artefact types for each raw material at
 273 Panda 100

	Diorite		Granite		Laterite		Quartzite		Total Assemblage	
	n	%	n	%	n	%	n	%	n	%
Group 1.1	1	11.1	13	3.5	0	0.0	0	0.0	14	3.0
Group 1.2	3	33.3	25	6.6	1	1.3	0	0.0	29	6.2
Group 2.1	0	0.0	1	0.3	0	0.0	1	16.7	2	0.4
Group 2.2	0	0.0	26	6.9	7	8.8	0	0.0	33	7.0
Group 2.3	1	11.1	0	0.0	0	0.0	0	0.0	1	0.2
Group 3	3	33.3	0	0.0	0	0.0	0	0.0	3	0.6
Group 4	0	0.0	18	4.8	7	8.8	0	0.0	25	5.3
Group 5	1	11.1	293	77.9	65	81.3	5	83.3	364	77.3
Total	9		376		80		6		471	

274

275

Table 3. Dimensional data for each percussive technological category at Panda 100

	Diorite				Granite				Laterite				Quartzite			
	Min	Max	Mean	St.Dev	Min	Max	Mean	St.Dev	Min	Max	Mean	St.Dev	Min	Max	Mean	St.Dev
Group 1.1	Length (mm)	34.6	34.6	34.6	41.0	13.5	-	-	-	-	-	-	-	-	-	-
	Width (mm)	15.9	15.9	15.9	17.5	53.3	31.9	11.1	-	-	-	-	-	-	-	-
	Thickness (mm)	9.0	9.0	9.0	11.0	49.9	26.4	10.9	-	-	-	-	-	-	-	-
Group 1.2	Weight (g)	7.8	7.8	7.8	5.3	108.4	38.5	34.8	-	-	-	-	-	-	-	-
	Length (mm)	42.9	112.5	67.8	38.8	23.5	83.9	47.3	16.9	93.4	93.4	93.4	-	-	-	-
	Width (mm)	19.0	82.6	42.9	34.6	18.3	74.1	35.0	13.3	52.1	52.1	52.1	-	-	-	-
Group 2.1	Thickness (mm)	16.0	46.8	26.5	17.6	12.7	42.7	23.6	7.6	50.1	50.1	50.1	-	-	-	-
	Weight (g)	18.4	303.3	116.0	162.3	7.6	200.9	47.2	46.2	322.9	322.9	322.9	-	-	-	-
	Length (mm)	-	-	-	-	36.8	36.8	36.8	-	-	-	-	77.0	77.0	77.0	77.0
Group 2.2	Width (mm)	-	-	-	-	26.3	26.3	26.3	-	-	-	-	44.9	44.9	44.9	44.9
	Thickness (mm)	-	-	-	-	16.9	16.9	16.9	-	-	-	-	31.4	31.4	31.4	31.4
	Weight (g)	-	-	-	-	16.0	16.0	16.0	-	-	-	-	124.9	124.9	124.9	124.9
Group 3	Length (mm)	-	-	-	-	20.2	79.1	33.1	14.2	25.4	77.6	50.5	20.2	-	-	-
	Width (mm)	-	-	-	-	12.3	61.3	24.6	12.2	15.2	64.6	38.4	20.3	-	-	-
	Thickness (mm)	-	-	-	-	6.9	35.9	17.2	7.0	12.2	55.3	30.1	17.0	-	-	-
Group 4	Weight (g)	-	-	-	-	2.3	159.6	23.1	39.0	2.8	217.9	85.0	88.8	-	-	-
	Length (mm)	39.2	39.2	39.2	-	-	-	-	-	-	-	-	-	-	-	-
	Width (mm)	28.8	28.8	28.8	-	-	-	-	-	-	-	-	-	-	-	-
Group 5	Thickness (mm)	8.9	8.9	8.9	-	-	-	-	-	-	-	-	-	-	-	-
	Weight (g)	8.6	8.6	8.6	-	-	-	-	-	-	-	-	-	-	-	-
	Length (mm)	27.2	49.7	36.4	11.8	-	-	-	-	-	-	-	-	-	-	-
Group 6	Width (mm)	14.0	44.2	27.5	15.4	-	-	-	-	-	-	-	-	-	-	-
	Thickness (mm)	6.3	15.8	10.0	5.1	-	-	-	-	-	-	-	-	-	-	-
	Weight (g)	3.2	33.4	14.2	16.7	-	-	-	-	-	-	-	-	-	-	-
Group 7	Length (mm)	-	-	-	-	12.5	67.7	25.3	12.5	17.1	58.6	39.1	14.0	-	-	-
	Width (mm)	-	-	-	-	9.6	60.1	19.2	11.2	15.8	43.6	32.7	10.1	-	-	-
	Thickness (mm)	-	-	-	-	4.9	31.5	12.4	5.7	6.5	27.5	19.4	8.0	-	-	-
Group 8	Weight (g)	-	-	-	-	.8	117.5	10.8	26.8	2.1	48.6	25.9	18.2	-	-	-
	Length (mm)	14.9	14.9	14.9	-	2.9	23.9	9.6	3.9	3.9	29.0	10.1	4.2	4.6	10.7	7.1
	Width (mm)	11.8	11.8	11.8	-	1.2	19.3	7.2	2.9	2.6	15.3	7.2	3.2	3.4	7.7	5.6
Group 9	Thickness (mm)	4.7	4.7	4.7	-	1.1	13.5	5.1	2.1	1.5	11.7	4.7	2.4	2.1	7.3	4.6
	Weight (g)	.8	.8	.8	-	.1	4.9	.5	.7	.1	4.3	.5	.8	.1	.9	.4

278 4.1.2 Quartzite assemblage

279 Six quartzite artefacts were recovered from the P100 excavations, two from the vicinity of Anvil 4, two
280 from Anvil 3 and one each from Anvils 5 and 6. Small debris makes up the majority of this sample
281 (n=5, 83.3%), with a mean length, width and thickness of 7.1 x 5.6 x 4.6 mm and a mean weight of
282 0.4 g (Table 3). The small debris does not show evidence of percussive damage, and as such may
283 represent a background natural 'noise' of small quartzite fragments.

284 A single tabular quartzite edge fragment was also identified, measuring 77 x 44.9 x 31.4 mm and
285 weighing 124.9 g (Table 3). This edge piece possesses a single impact point located on the intersection
286 of a cortical horizontal plane and a newly fractured vertical plane. The fractured pane is clearly non-
287 cortical and possesses sharp and fresh edges, indicating it as a relatively recent breakage. Apart from
288 the impact point that resulted in the fragmenting of the hammerstone, no repeated percussion marks are
289 evident on either horizontal planes of the edge fragment. However, it has been shown that very little
290 macro and microscopic damage develops on quartzite during nut cracking activities (de la Torre et al.,
291 2013), which may go some way to explaining the lack of visible percussive damage, coupled with the
292 fact that softer organic anvils were used at this site. The thickness of this piece (31.4 mm) suggests that
293 the original hammerstone was probably relatively thin.

294

295 4.1.3 Diorite assemblage

296 Eight diorite artefacts have a total weight of 407.7g. Almost all were found around Anvil 4 (n=7,
297 87.5%), with a single fragment from Anvil 1. The diorite artefacts include corner (n=3, 33.3%) and
298 edge fragments (n=1, 11.1%), typical hammerstone flakes (Group 3) (n=3, 33.3%), a conchoidally
299 fractured piece or positive base (n=1, 11.1%), and a single piece of small debris (11.1%). Compared to
300 the dominant granitoid raw material at P100, the diorite is relatively homogenous in structure, with no
301 visible internal fissures or fractures and a fine-grained texture. The higher quality of this raw material
302 helps explain the high percentages of fractured diorite pieces as opposed to angular chunks and small
303 debris.

304 The single diorite edge fragment measures 34.6 x 15.9 x 9 mm (maximum dimensions) and weighs
305 7.8 g (Table 3), however when orientated technologically this fragment is relatively wide and thin in
306 morphology (15.6 x 33.8 mm). All diorite corner fragments retain a portion of the active percussive
307 plane, indicating that this surface was flat and cortical (Figure 2B). In addition, Refit Set 2 (see below)
308 is a distal fragmentation of a corner piece that retains both the active percussive plane and the opposed
309 plane (Plane A2) suggesting that the diorite hammer had a tabular morphology. Coupled with the
310 presence of typical hammerstone flakes (see below), two distinct morphologies of diorite hammerstone
311 were used, tabular blocks and rounded cobbles. The majority of diorite percussive fragments possess a

312 cortical dorsal surface, with only a single example possessing a fully non-cortical dorsal surface. This
313 finding suggests that repeated fragmentation of individual diorite hammerstones was a rare occurrence.

314 Of particular interest amongst the diorite artefacts is the singular piece that resembles, morphologically,
315 a percussive flake (Figure 3). This piece possesses a clear non-cortical striking platform, although no
316 distinct impact points are visible. The striking platform is relatively large, measuring 7.5 x 16.5 mm
317 with a flat morphology. The flake possesses clearly delimited dorsal and ventral surfaces and a diffuse
318 bulb of percussion. The dorsal surface is >50% cortical, however it also retains evidence of three
319 previous unidirectional, small dorsal removals. However, it is impossible to identify whether these
320 removals were flake detachments or merely evidence of previous fragmentation.

321 Three of the diorite fragments can be considered stereotypical hammerstone detachments, two complete
322 and one fragmented (Figure 3). These possess convex cortical dorsal surfaces with highly concave
323 ventral surfaces. No clear impact point is present and none possess an area that could be considered a
324 striking platform.

325

326 **Insert Figure 2**

327 **Figure 2.** Examples of detached percussive products from lithic hammerstones at P100. (A) Granitoid
328 and diorite edge pieces (Group 1.1). (B) Granitoid and diorite corner fragments (Group 1.2). (C)
329 Examples of granitoid and laterite small debris (<20 mm) (Group 5) (scales = 5 cm).

330

331 **Insert Figure 3**

332 **Figure 3.** Examples of detached percussive artefacts from lithic hammerstones at P100. (A) Detached
333 diorite conchoidal flake (Group 2.3). (B) Detached diorite typical hammerstone flakes (Group 3) (scales
334 = 5 cm)

335

336 4.1.4 Laterite assemblage

337 80 laterite fragments, weighting a total of 1131.9 g, were found at P100. Most of these are either small
338 debris (n=65, 81.3%) or angular chunks and fragments (Group 2.2 and Group 4) (n=14, 17.6%), along
339 with a corner fragment (n=1, 1.3%), with no clear evidence of percussive behaviour other than their
340 fragmented state. Of note, the single corner fragment and an angular chunk were found to refit (Refit
341 Set 9), which provides the only potential evidence of percussive behaviour for this material and is
342 described in detail below. A second refit (Refit Set 1) records the fracturing of a small laterite cobble,
343 which was likely not used for successful *Panda* nut percussion, however, may have been used by a

344 juvenile (Boesch and Boesch, 1984b). The lack of macroscopic percussive damage on the majority of
345 laterite artefacts does not in itself necessarily preclude laterite being used in percussive behaviour. Their
346 close association with organic anvils and nut shells, coupled with the fact that chimpanzees in Taï have
347 been known to use this raw material, all increase the possibility of a percussive origin for these artefacts.
348 However, based purely on percussive damage evidence in the P100 archaeological context this raw
349 material would not be attributed to percussive behaviour. These laterite pieces represent the
350 fragmentation or splitting of relatively small cobbles, and they do not share the same morphology as a
351 detached corner fragments from a larger tabular block, as is seen with the diorite hammerstones.

352

353 4.1.5 Granitoid assemblage

354 The 376 granitoid artefacts make up the majority of the P100 lithic assemblage. The P100 granitoid is
355 coarse-grained, with a high quartzite composition in the form of individual crystals held in a fine grained
356 matrix. Its internal structure has major fractures and fissures directly associated with regions of interior
357 foliation that often grade into a highly irregular, coarse-grained internal structure.

358 The majority of the granitoid pieces are small debris (n=293, 77.9%) (Figure 2) with mean dimensions
359 of 9.6 x 7.2 x 5.1 mm and a mean weight of 0.5 g (Table 3). The second most prevalent artefact types
360 are angular chunks and angular fragments (including groups 2.1, 2.2 and group 4) (n=45, 12%); these
361 show no evidence of percussive damage but their highly fragmented state suggests a percussive origin.
362 Of the identifiable percussive techno-morphological categories, corner fragments are the most frequent
363 (n=25, 6.6%), followed by edge fragments (n=13, 3.5%). The presence of these technological morpho-
364 types within the assemblage represents archaeologically visible evidence of percussive behaviour, and
365 in a number of cases these artefacts possess direct evidence of percussive impact.

366 The corner fragments possess mean maximum measurements of 47.3 x 35 x 23.6 mm and a mean weight
367 of 47.2 g (Table 3). When orientated technologically, however, they possess a mean length and width
368 of 35.2 x 37.8 mm, presenting a roughly cuboid morphology. The preserved portion of the active
369 percussive plane (platform) was identifiable in 92% (n=23) of all corner fragments. The majority
370 possessed cortical platforms (n=19, 76%), however, a small number also possessed fully non-cortical
371 platforms (n=3, 12%). These platforms were relatively large (average length and width: 25.3 x 17.6mm)
372 and flat. Granitoid corner fragments possess relatively large external (mean = 122.7 degrees) and
373 interior (mean=102.5 degrees) platform angles, highlighting the forceful nature of their detachment.
374 Corner fragments possessed either flat (n=13, 52%) or irregular (n=10, 40%) ventral surface
375 morphologies, with only a very small proportion possessing concave morphologies. Dorsal surfaces
376 were primarily >50% cortical (>50-100% cortex coverage) (n=21, 84%), with only a few examples
377 possessing <50% cortex coverage (n=4, 16%) (Figure 2). Only 12% (n=3) possessed dorsal surface
378 detachments, suggesting that corner fragment detachment often occurred as an initial breakage of the

379 hammerstone. These fragments also typically possessed either a triangular (n=14, 56%) or trapezoid
380 (n=9, 36%) transversal cross section.

381 Granitoid edge fragments possess mean maximum measurements of 41 x 31.9 x 26.4 mm and a mean
382 weight of 38.5 g (Table 3). However, when technologically orientated they measure on average 28.6 x
383 32.5 mm, making them relatively wide and short in morphology. Almost all possess a fully cortical
384 (n=12, 92.3%) striking platform or the remnants of the active percussive plane, with only one example
385 (7.7%) possessing a non-cortical platform. The platforms are relatively substantial and rectilinear in
386 morphology, possessing a mean length and width of 28.2 x 21.4 mm. Edge fragments possessed a mean
387 exterior platform angle of 117.7 degrees and a mean interior platform angle of 98.5 degrees. The dorsal
388 surfaces of these fragments, representing the outer plane of the hammerstone, possess either triangular
389 (n=5, 38.5%) or trapezoid (n=8, 61.5%) transversal cross section, and are rarely fully cortical (n=1,
390 7.7%) or non-cortical (n=1, 7.7%), possessing either >50% (n=7, 53.8%) or <50% cortex coverage
391 (n=4, 30.8%) (Figure 2). The presence of non-cortical regions on the dorsal surface, coupled with the
392 identification of single dorsal extractions on four (30.8%) pieces, suggests that there is a repeated nature
393 to the edge fragmentation of the P100 granitoid hammerstones.

394

395 *4.2. Refit analysis*

396 The original Panda 100 publication reported seven refit sets, totalling 16 refitted artefacts, and
397 comprising three raw materials: granitoid, laterite and diorite (Mercader et al., 2002). These refits
398 revealed a maximum horizontal movement of 1.6 m and were identified at two of the six excavated
399 anvil locations, Anvils 1 and 4. The original report did not identify the artefacts that contributed to these
400 refit sets, with only one refit being identified via an illustration (Mercader et al., 2002 Fig. 2E). No
401 technological analysis of the refitted material was presented.

402 Our updated refit analysis of the Panda 100 lithic assemblage substantially increases the number of
403 refits, and provides a detailed technological analysis of each refit set (Supplementary Material 2). A
404 total of 35 artefacts were refitted (7.43% of the entire assemblage), increasing the total number of refit
405 sets from seven to twelve (Table 4). Other than the illustrated example in Mercader et al. (2002), we do
406 not know which of the refits identified in this study overlap with the ones described in the original
407 report. The increased number of refit sets does, however, permit a number of new insights. First, refits
408 are now represented at four separate anvil locations: while the majority are located within the vicinity
409 of Anvil 4, refits are also identified at Anvils 1, 2, and 5. Second, three of the refit sets represent
410 movement of hammerstones between anvil locations, with refitted fragments being identified between
411 Anvil 4 and Anvils 1 and 5 as well as between Anvils 2 and 5.

412 The refits illustrate how hammerstones fragment during *Panda* nut cracking behaviour (Figures 4-8).
413 The majority of the large fractures result from detachment of corner and edge fragments, often in
414 tandem, with these pieces being detached consecutively or simultaneously. It is, however, possible to
415 identify two primary fragmentation sequences within the P100 refits. The first sequence consists of
416 small, non-invasive removals that detach a small portion of the intersection between the horizontal
417 active plane and the vertical planes. This type of hammerstone fragmentation results in an increasingly
418 rounded morphology of the hammerstone edges. The second fragmentation sequence is a more invasive
419 ‘slicing’ of the hammerstone, whereby a large corner or edge fragment that retains remnants of both the
420 active percussive surface, as well as the opposing plane of the hammerstone, is detached. This process
421 results in a rapid loss of the volume of the hammerstone. Both of these fragmentation sequences are
422 represented within the refit assemblage independently, as well as associated with each other in single
423 refits sets. Furthermore, corner fragments appear to result from initial fragmentation of the
424 hammerstone, followed either simultaneously or soon afterwards by detachments of short and wide
425 edge fragments.

426

427

428

429

430

431

432

433

434

435

436

437

438

439

440

441

442 **Table 4.** Refits identified in the current study of the Panda 100 lithic assemblage

Refit Set	Raw Material	Number of Pieces	Piece Numbers	Technological Categories	Grid Reference	Total Horizontal Distance (m)	Spit Range
1	Laterite	2	P15	2.2	R9	0.21	1-2
			P16	2.2	R9		
2	Diorite	2	P25	1.2	S10	1-2*	0-1
			P7	1.1	R11		
3	Granitoid	4	P28	1.2	S10	9.54 ¹	1-2
			P29	1.1	S10		
			P39	1.1	K7		
			P47	1.2	K8		
4	Granitoid	2	P40	1.2	K7	1-2*	3
			P53	1.1	K8		
5	Granitoid	2	P18	2.2	S10	1.27	0-1
			P42	2.2	R11		
6	Granitoid	3	P48	1.2	T10	0.26	0
			P52	1.2	T10		
			P97	2.2	T10		
7	Granitoid	4	P12	1.2	S10	1.34	0-1
			P30	1.1	T10		
			P32	1.2	?		
			P45	1.2	S10		
8	Granitoid	2	P49	1.2	T10	0.83	0
			P51	1.1	S10		
9	Laterite	2	P21	1.2	N6	17.12 ¹	1
			P33	2.2	L23		
10	Granitoid	5	P6	1.1	R10	16.59 ¹	0-1
			P9	1.2	K24		
			P22	2.2	T10		
			P27	1.2	R10		
			P56	4	S10		
11	Granitoid	2	P1	1.2	T10	-	-
			P11	1.2	?		
12	Granitoid	5	P24	1.1	L8	1.49	1-3
			P41	1.1	K8		
			P58	2.2	K8		
			P65	2.2	K8		
			P88	4	K8		

443 * No direct measurement possible for entire refit sequence, distance was estimated based on grid
 444 reference

445 ¹ No direct measurement possible for a single piece in refit set, distance was estimated based on grid
 446 reference

447

448

449

450

451 **Insert Figure 4**

452 **Figure 4.** Refit Sets 1 and 2 from Panda 100. (A) Refit Set 1: Two laterite angular chunks. (B) Refit
453 Set 2: Distally fractured, detached corner fragment of a diorite hammerstone (scales = 5 cm)

454

455 **Insert Figure 5**

456 **Figure 5.** Refit Sets 3 and 4 from Panda 100. (A) Refit Set 3: Four granitoid fragments, two edge
457 fragments and two corner fragments. (B) Refit Set 4: Two granitoid fragments representing a corner
458 region of a hammerstone (scales = 5 cm)

459

460 **Insert Figure 6**

461 **Figure 6.** Refit Sets 5, 6 and 7 from Panda 100. (A) Refit Set 5: Two angular chunks representing the
462 edge of a granitoid hammerstone. (B) Refit Set 6: Two corner fragments and one angular chunk
463 representing corner detachment of a granitoid hammer. (C) Refit Set 7: Corner refit of a tabular granitoid
464 hammerstone consisting of three corner fragments and one edge fragment (scales = 5 cm)

465

466 **Insert Figure 7**

467 **Figure 7.** Refit Sets 8 and 9 from Panda 100. (A) Refit Set 8: Edge fragment of a granitoid hammerstone
468 consisting of one corner fragment and one edge fragment. (B) Refit Set 9: Minor fragmentation of a
469 laterite cobble (scales = 5 cm)

470

471 **Insert Figure 8**

472 **Figure 8.** Refit Sets 10, 11, and 12 from Panda 100. (A) Refit Set 10: Five granitoid fragments (three
473 corner fragments, two angular chunks) representing extensive fragmentation of a large hammerstone.
474 (B) Refit Set 12: Five granitoid fragments (two edge fragments, three angular chunks) of a larger
475 hammerstone corner region. (C) Refit Set 11: Edge fragment of a granitoid hammerstone consisting of
476 one angular chunk and one edge fragment (scales = 5 cm)

477 4.2.1 Spatial analysis: refitted data

478 Just under half of the P100 refit sets (n=5, 41%) are formed of pieces from two neighbouring meter
479 squares at the site, and therefore represent a horizontal movement of 1-2 m. A smaller number come
480 from the fragmentation of a hammerstone within a single meter (n=3, 25%), or a horizontal movement
481 of <1 m. However, three (25%) refit sets record more substantial horizontal movement and inter-anvil
482 transportation of hammerstones. In one instance, the hammerstone was transported 9.54 m between
483 successive breakage events, and in two instances refitting pieces were found 16-17 metres apart (Figure
484 9 and Figure 10) (Supplementary Material 3).

485 Four refits (33%) record hammerstones that were likely broken at a single point in time, with examples
486 found within the subsurface level and Spits 1 and 3 respectively. Another four refits were found between
487 the subsurface level and spit 1, with a further two (17%) examples being identified between Spits 1 and
488 2, representing a maximum vertical movement of 6cm. A single refit (8%) was formed of pieces found
489 in Spits 1-3, representing a maximum vertical movement of 9cm. This vertical movement suggests a
490 degree of reuse of hammerstones over time, with previously used hammerstones being actively removed
491 from the developing archaeological record and subsequently fragmented.

492

493 **Insert Figure 9**

494 **Figure 9.** Spatial map of Panda 100 excavations showing refit sets

495 **Insert Figure 10**

496 **Figure 10.** Mapped artefacts and refit sets at Panda 100, separated by anvil and spit

497

498

499

500

501

502

503

504

505

506

507

508

509 *4.2 Microscopic analysis*

510 Microscopic damage was identified on 13 fragmented pieces (Table 5). Most of these were corner
 511 fragments (n=9, 69.2%), however, edge fragments (n=4, 30.8%) are also represented (Table 5).
 512 Granitoid is the prevalent raw material, making up eight of the 13 pieces with visible percussive
 513 damage, whereas only a single diorite artefact possessed visible percussive wear.

514

515 **Table 5.** Percussive damage identified on lithic artefacts from P100

Piece Number	Raw Material	Artefact Category	Microscopic Percussive Damage
P13	Granitoid	1.2	Crushing and levelling of individual crystals. The development of a frosted and irregular surface morphology.
P14	Diorite	1.2	Isolated crushing and fracturing of individual quartz crystals Large area of intense crushing of quartz crystals and matrix.
P31	Granitoid	1.2	Development of large step scars and the detachment of individual crystals.
P37	Granitoid	1.2	Small areas of crushing, and frosting of quartz crystals. Small step fractures within the crushed areas
P38	Granitoid	1.2	Crushing of quartz crystals and surrounding matrix. Detachment of individual crystals and the development of step scars.
P48	Granitoid	1.2	V-shaped impact point in close association with intense crushing of quartz crystals.
P70	Granitoid	1.1	V-shaped impact point. Intense crushing of quartz crystals and light crushing of matrix. Levelling of quartz crystals, resulting in an irregular surface morphology.
P80	Granitoid	1.2	V-shaped impact point, associated with an area of crushing and levelling of quartz crystals. Detachment of individual crystals from the matrix, and the development of small step scars.
P91	Granitoid	1.2	V-shaped impact points, associated with intense crushing of quartz crystals and matrix. Small step fractures.
P41	Granitoid	1.1	Small area of crushed quartz crystals and matrix
P24	Granitoid	1.1	Isolated area quartz crushing and slight pitting of the surface
P39	Granitoid	1.1	Small area of crushed quartz crystals and matrix
P47	Granitoid	1.2	Small area of crushed quartz crystals and matrix
P25	Diorite	1.2	No identifiable percussive damage

516

517 Undamaged cortical granitoid surfaces are light brown with frequent, large, intact quartz crystals. The
518 natural granitoid surface morphology is either flat and levelled (with the quartz crystals showing worn
519 dulled surfaces) or, conversely, highly irregular (with protruding quartz crystals representing high
520 points on the surface). Percussive damage on granitoid hammerstone fragments is generally sparsely
521 located on the active percussive surface. The impacts are either located towards the centre of the
522 percussive plane or immediately on the edge where the percussive plane intersects one or more vertical
523 outer planes.

524 At a macroscopic level, percussive damage can be identified as a differentiation in colour when
525 compared to the unaltered cortical surface. At a microscopic level, percussive damage on these pieces
526 is characterised by crushing of individual grains, resulting in a compacted or compressed morphology
527 located around a single impact point. This crushing and compaction results in a discolouration or
528 frosting of the cortical surface to a distinct white. When impacts are located close to the edge they
529 present a characteristic V-shape in plan, whereas, when located in the centre of the active plane on a
530 relatively flat surface, they are characterised by an irregular plan shape. When located along an
531 intersecting edge impacts may also be associated with either a single large step-terminating removal or
532 a series of smaller crushed step fractures, where individual quartz crystals have either detached or
533 fragmented. Whole quartz crystals may be detached from the granitoid matrix, leaving behind
534 characteristic, deep depressions surrounded by an area of crushed and compacted matrix. These
535 characteristics either occur individually or as combinations, and appear to be influenced by the density
536 of quartz crystals within the granatoid matrix (Figure 11 and Figure 12).

537 Percussive damage on the single diorite artefact is superficial and only identifiable through macroscopic
538 visual inspection by a slight depression and roughening of the cortical surface. Under the microscope,
539 few identifiable characteristics can be clearly contrasted to the non-damaged cortical surfaces. Two
540 small impact points and areas of crushing of the quartz crystals can be identified within the wider
541 depressed area, however, these are not clearly related to percussive damage.

542 The issue of identifying percussive damage on diorite fragments at P100 is further complicated by the
543 larger corner fragment from Refit Set 2. Originally illustrated in Mercader et al (2002, Fig. 2E), this
544 piece possesses a small visible depression on its horizontal active plane (Plane A) measuring 26 x
545 15 mm in maximum dimensions. This has been interpreted as pitting (Mercader et al, 2002), however,
546 it is a natural undulation of the cortical surface. The lack of significant microscopic percussive traces
547 within the depressed region of the active plane indicates that this area was not formed through active
548 use. This is not to suggest that this artefact, and indeed the associated refit set, is not derived through
549 chimpanzee percussive action, only that the previously identified pitted feature is a natural depression
550 within the surface morphology of the hammerstone (Figure 12).

551

552

553 **Insert Figure 11**

554 **Figure 11.** Microscopic damage on percussive artefacts at Panda 100. (A) Granitoid corner fragment
555 (Group 1.2) with clear percussive damage. 1 and 2: Cortical, undamaged areas, showing intact quartz
556 crystals and flat smooth surface (scales = 500 μm and 1000 μm). 3 and 4: Impact point showing
557 significant crushing and development of small steps along with detachment of quartz crystals (scales =
558 500 μm and 1000 μm). (B) Granitoid edge fragment (Group 1.1). 1: Undamaged cortical surface (scale
559 = 500 μm). 2, 3 and 4: V-shaped impact points along the edge and interior of the percussive surface
560 (scales = 3000 μm , 3000 μm and 500 μm)

561

562

563 **Insert Figure 12**

564 **Figure 12.** Microscopic damage of percussive artefacts at Panda 100. (A) Granitoid corner fragment
565 with clear percussive damage. 1: Cortical, undamaged surface (scale = 500 μm). 2: V-shaped impact
566 point (scale 1000 μm). 3: Crushing and step fractures associated with impact point (scale = 3000 μm).
567 4.: Impact point showing significant crushing of quartz crystals and matrix (scale = 1000 μm). (B)
568 Diorite corner fragment with possible pitted surface. 1 and 2: Cortical, undamaged surfaces preserving
569 intact crystals and matrix. 3 and 4: Undamaged surface from within the pitted surface, showing intact
570 crystals and matrix (scale = 2000 μm).

571

572 **4. Discussion and conclusions**

573 Panda 100 was the first site to be archaeologically excavated to recover tool non-hominin tools.
574 However, the site has much to offer beyond its historical significance. It provides the highest resolution
575 data available on how non-human animals create an archaeologically durable assemblage, giving new
576 insights into how wild chimpanzee stone tools break and move during their use under natural conditions.

577 The P100 artefacts conclusively demonstrate that there is a disconnect between the stone pieces left at
578 *Panda* nut-cracking sites and the actual hammers used by chimpanzees to crack nuts. The former are
579 fragmentary and small, the latter are large and battered. P100 therefore preserves evidence for an
580 important behavioural observation made at Tai, namely that hammerstones are routinely removed from
581 a site when a *Panda* tree becomes unproductive or dies. The P100 archaeological record has a
582 preservation bias against actual tools, and towards stone pieces that could not in themselves ever be
583 used to crack *Panda* nuts. Given that the evolution of chimpanzee stone technology likely encompasses
584 at least tens of thousands of years [Add Haslam 2014 American Journal of Primatology here], with tool

585 use potentially reaching into the millions of years (Panger et al., 2003), the correct interpretation of
586 partial behavioural evidence at sites like P100 is critical for reconstructing that long-term record.

587 The raw materials excavated at the P100 site – granitoid, laterite, diorite and quartzite – accurately
588 reflect the materials that primatologists have observed chimpanzees using for *Panda* processing in the
589 Taï Forest (Boesch and Boesch, 1983). Other than laterite, these stones do not occur naturally in the
590 immediate vicinity of the site, demonstrating that they were transported by chimpanzees. This kind of
591 transport, essentially provisioning the *Panda* tree while it fruits, has also been well documented at Taï
592 (Boesch and Boesch, 1984a; Luncz et al., 2016). In themselves, therefore, the fragmented P100 artefacts
593 permit reconstruction of such fundamental behaviour as material selection and tool transport. From a
594 primate archaeological perspective this is important as it allows the reconstruction (albeit at a low
595 resolution) of primate behaviour in antiquity. In addition, GIS mapping of artefacts to their grid
596 reference shows that the highest concentrations of material are found within the immediate vicinity (<1
597 m) of anvils (Figure 13). If the aim is to maximise recovery of artefacts, future West African chimpanzee
598 archaeological excavations may therefore wish to concentrate on areas around anvils.

599

600

601 **Insert Figure 13**

602 **Figure 13.** Density maps of artefacts at Panda 100, separated by anvil location

603 Our technological analysis of the P100 artefacts is the most detailed yet performed for a wild
604 chimpanzee lithic assemblage. It allows us to describe and interpret details of the unintentional
605 reduction of stone tools by chimpanzee nut-cracking at a high resolution. This analysis found that two
606 main fragmentation sequences dominate at P100, which may occur either independently, or
607 concurrently. First, protruding corner regions of a hammerstone are removed through either direct
608 impact or initiation of internal fracture planes. From behavioural observations, we know that such
609 impacts are not deliberately aimed at the tool margins, but instead represent mis-hits or incidental blows,
610 such as when the hammer contacts the anvil during nut-cracking (Arroyo et al., 2016). Once corner
611 elements are removed, edge fragments (the intersection of two planes) are then susceptible to breakage.
612 These removals are non-invasive, and this process sequentially rounds the sharp edges and corners of
613 an originally angular hammerstone, reducing its mass but not significantly reducing its overall size with
614 each fragmentation event. This fragmentation may occur recurrently, as shown by non-cortical dorsal
615 surfaces of detached edge fragments.

616 The second fragmentation sequence involves the wedging initiation or ‘slicing’ of tabular pieces, in
617 which portions of both the active hammer surface and its opposing surface are removed at the same
618 time. It occurs either because of excessive force used during the hammer strike (compared to the force

619 required to simply remove a protruding corner or edge), or because of the presence of internal fracture
620 planes. This process decreases both the mass and the size of a hammer, which if continued will reduce
621 the stone to a form where it is no longer suitable for use as a *Panda* hammer. Further, this reduction
622 sequence allows for an estimate of the original hammerstone thickness, because of the preservation of
623 opposing hammer faces. Both of the main fragmentation sequences are present in the refit sets at P100,
624 which means that they can be reconstructed in detail from the preserved archaeological evidence, even
625 if direct observations were unavailable.

626 As noted, the lack of complete hammerstones is the most striking feature of the P100 assemblage. This
627 absence is remarkable considering that the assemblage consists of more than 400 artefacts, accumulated
628 over a period of at least 21 years from a known *Panda* nut-cracking site. In some cases, usable hammers
629 may have been completely fragmented, particularly if they were made of the more fragile granitoid and
630 laterite materials. However, the extensive refitting efforts made in the current study, which almost
631 doubled the number of known refits from P100, demonstrate that such a scenario is untenable for the
632 large majority of recovered artefacts. The diorite assemblage is the most informative in this regard, as
633 it is composed of a distinct and relatively fine-grained material that is easily recognised and allows for
634 clear reconstruction of percussive activities - for example, the only conchoidal flake at P100 is a diorite
635 piece. There are no diorite artefacts of sufficient size or mass to crack *Panda* nuts, which require
636 hammerstones of 1-9 kg (Boesch and Boesch, 1983). The logical conclusion, therefore, is that any such
637 tools have been moved offsite by the chimpanzees. Interestingly, at least part of this movement was
638 completed by the chimpanzees in the relatively short five-year gap between the death of the *Panda* tree
639 at P100 and its excavation. Furthermore, the exclusive recovery of small hammerstone fragments and
640 the lack of complete or even substantial fragments of *Panda* nut hammerstones in the P100 record
641 suggests that an exclusive focus on complete or broken hammerstones is not adequate when dealing
642 with the behavioural prehistory of chimpanzee groups.

643 Chimpanzee tool transport is also recorded in the refit analysis. We have identified refitted pieces
644 separated by 16-17 m at the time of excavation, representing the longest known instance of such
645 movement in the excavated primate archaeological record. In addition, the present study found the first
646 archaeological evidence of movement of a single hammerstone between two separate nut cracking
647 locations. While this is unsurprising given the well-known chimpanzee transport of hammers in the Taï
648 Forest (Boesch and Boesch, 1984a; Luncz et al., 2016), the fact that such behaviour is preserved and
649 recoverable from the primate archaeological record is promising for studies conducted at sites where
650 animals are either unobserved or no longer present.

651 Wild chimpanzee hammerstone movement has been examined under experimental conditions by
652 Carvalho et al. (2008) in Guinea. By observing and mapping the movement of hammerstones and
653 portable anvils provided for the animals by human experimenters, it was shown that chimpanzee oil

654 palm nut cracking hammerstones may undergo a number of different movement sequences within a
655 local area (Carvalho et al., 2008). They noted, however, that the indirect record, i.e., the final resting
656 place of a chimpanzee hammerstone, does not provide data on its previous use location(s). They suggest
657 that hammerstone use-life can be better understood by using direct observational data derived from
658 primatological studies. In contrast, the results of our current study show that sufficiently fine-grained
659 archaeological data on hammerstone fragments, including spatial and technological analysis, offer a
660 reliable additional means for reconstructing the minimum individual movements of a hammerstone
661 within a chimpanzee nut cracking site. This finding has the potential to allow the tracing of diachronic
662 behavioural variation through the primate archaeological record, including, potentially detailed
663 hammerstone use sequences at a local and regional (Luncz et al., 2016) scale. In addition, given
664 sufficient sample size and differentiation between raw materials, it may be possible in future studies to
665 identify a minimum number of hammerstones use at a given location.

666 In a wider context, since P100 was first published there have been excavations of stone tool activity
667 areas for two more non-human primate species: Burmese long-tailed macaques (*Macaca fascicularis*
668 *aurea*) in Thailand and bearded capuchin monkeys (*Sapajus libidinosus*) in Brazil (Haslam et al., 2016a,
669 2016b; Proffitt et al., 2016). Along with P100, these sites reveal a diversity of primate site formation
670 processes, derived from both behavioural and environmental factors. For example, the rarity of suitable
671 *Panda* hammerstones at Taï mirrors the situation for the wild capuchins at the Fazenda Boa Vista site
672 (Visalberghi et al., 2009). In both cases, heavy but scarce hammers are required to crack tough nuts,
673 and these hammers are not left at abandoned sites for a sufficient length of time to readily enter the
674 archaeological record (Visalberghi et al., 2013). In contrast, wild capuchins at Serra da Capivara
675 National Park (SCNP) (Haslam et al., 2016b) and wild macaques at Laem Son National Park (Haslam
676 et al., 2016a) have abundant material suitable for use as hammerstones, with the result that these enter
677 the archaeological record at a sufficient rate to enable later recovery.

678 Fragmentation of the Taï stone material occurs through a combination of large forces during nut-
679 cracking and the natural weakness of the rock types employed by chimpanzees. The internal structure
680 of the hammerstone may become more susceptible to fracturing due to the development of internal
681 fracture planes, particularly evidence in granitoid. Additionally, hammerstones most frequently
682 fragment along the edges away from the primary use area, the centre of mass (Boesch and Boesch,
683 1983). This combination creates an archaeological assemblage that is essentially exclusively fragments,
684 a collection of abundant, small, fractured pieces that currently has no direct parallel in the nut-cracking
685 sites of other wild primates or hominins.

686 The discovery of stone tool flaking behaviour among the capuchins at SCNP (Proffitt et al., 2016) may
687 provide a more suitable comparative dataset for the emergence hominin flake technology. In the latter
688 instance, capuchins pound quartzite stones directly onto other stones to break down the tool surface,

689 producing many small flakes and angular pieces in the process. Despite potential similarities in debitage
690 density between the SCNP and chimpanzee sites, however, there is an important difference, in that the
691 capuchins regularly create conchoidally fractured, sharp-edged flakes, whereas the Taï chimpanzees do
692 not. This difference is likely mediated in part by the difference in percussive behaviour (stone-on-stone
693 percussion vs nut cracking) and raw material availability and quality.

694 The P100 lithic material, and chimpanzee nut cracking behaviour in general, has been argued to be of
695 importance in understanding early hominin percussive activities (McGrew, 1992; Mercader et al., 2007,
696 2002; Panger et al., 2003). As discussed earlier, by comparing the dimensions of fragmented pieces to
697 known Oldowan flakes and cores, Mercader et al. (2002) linked the lithic material produced at Panda
698 100 with the flaking technology of early hominins. Furthermore, similar comparisons have been made
699 between chimpanzee technology and hominin flaking elsewhere (Kortlandt, 1986; Marchant and
700 McGrew, 2005; McGrew, 1992).

701 Our analysis of the P100 hammerstone reduction sequences and the technological analysis of the
702 detached products highlights their unsuitability for direct comparison with intentional hominin knapped
703 assemblages (de la Torre, 2010). The earliest hominin stone tool technology (Lomekwian), as well as
704 all Oldowan lithic assemblages, indicate the intentional, repeated production of conchoidally fractured
705 flakes (de la Torre, 2004; Delagnes and Roche, 2005; Harmand et al., 2015; Lewis and Harmand, 2016;
706 Semaw et al., 1997). For the Oldowan, associated cores retain evidence of both simple and highly
707 structured exploitation strategies, often adhering to flaking rules. In addition to this, ESA knappers were
708 able to identify and rectify simple accidents and maximise the number of flakes per core through
709 directed hammerstone impacts and advantageous use of naturally occurring angles (Delagnes and
710 Roche, 2005; Semaw, 2000; Stout et al., 2010). The rarity at P100 of conchoidal flakes (0.002%),
711 coupled with the highly restricted and incidental range of fragmentation patterns prevent this
712 assemblage from being directly comparable to even the simplest of Oldowan flaked assemblages. All
713 detached pieces identified in this study are associated with the forceful and accidental interaction of the
714 hammerstone with the passive anvil or the hard *Panda* nut target, with no instances of artefacts that
715 resemble knapping cores.

716 To a large extent the degree of hammerstone fragmentation is dictated by the overall quality of the
717 available raw material. Granitoid, for instance is highly fragmentary with numerous internal fractures,
718 resulting in a high frequency of shatter even when used against soft organic anvils. On the other hand,
719 diorite hammerstones are far more homogenous, with fewer internal fractures, resulting in a
720 significantly reduced fragmented assemblage. Furthermore, the density of material in the excavated
721 areas at P100, initially likened to the densities seen at ESA archaeological sites (Mercader et al., 2002),
722 is largely mediated by the poor quality and highly fragmentary nature of the prevailing raw material,
723 granitoid, whereas the density of Oldowan sites is the consequence of intentional repeated flake

724 production. Having said this, however, the fragmentation of the Panda 100 assemblage offers an
725 opportunity to develop testable hypotheses regarding the use of organic anvils in the archaeological
726 record. Most of the chimpanzee material can be classified as small debris and percussive technological
727 categories, which cluster within the immediate vicinity of a used wooden anvil. It may, therefore, be
728 hypothesised that similar technological compositions and spatial clustering within the hominin
729 archaeological record, where there is a lack of stone anvils, may have been a consequence of organic
730 anvil use; an otherwise archaeologically invisible behaviour.

731 The lack of viable hammerstones in the P100 archaeological record acts as a primate analogy for the
732 high likelihood that both active hominin cores and hammerstones may not enter the archaeological
733 record at the location of their use. This analogy applies directly to those stones that were still adequate
734 for exploitation or percussive behaviour. A greater understanding of chimpanzee tool life histories will
735 likely help generate further insights into the apparent dichotomy between the frequency of identified
736 and expected flakes within certain hominin archaeological lithic assemblages (De la Torre and Mora,
737 2005; McNabb, 1998). To aid in this work, we will need additional technological and microscopic use
738 wear characterisations to those presented in this study, in association with complementary experimental
739 studies (Benito-Calvo et al, 2015; Arroyo, 2015; Arroyo et al., 2016; De la Torre et al., 2013). By
740 identifying similar mechanical processes underlying percussive damage, we will be better able to
741 identify and discriminate similar percussive behaviours in the ESA archaeological record. Ultimately,
742 our study shows that a lack of complete stone hammerstones or anvils in the archaeological record does
743 not necessarily preclude the presence of non-flaking percussive behaviour.

744 The P100 lithic assemblage represents an important dataset for investigating hominin percussive
745 behaviour (Mora and de la Torre, 2005). Artefact categories previously associated with hominin
746 percussive behaviour in the ESA archaeological record (Arroyo and de la Torre, 2016; De la Torre and
747 Mora, 2005; Mora and de la Torre, 2005) are represented at P100. This finding corroborates the
748 technological validity and cross-species viability of this classification system, and suggests that these
749 technological classificatory groupings are valid across different raw materials, and potentially raw
750 material qualities. In addition, this study has shown that technological categories typically associated
751 with anvil breakage may enter the archaeological record as a consequence of hammerstone breakage,
752 and if identified should not be inherently associated with percussive anvil breakage. The issue of
753 hammerstone breakage on organic (wooden) anvils has received little attention in the archaeological
754 literature, and may require further investigation given its presence - albeit as a minority feature - in the
755 primate tool use repertoire.

756 Our re-analysis of the first primate chimpanzee archaeological assemblages significantly updates our
757 knowledge of both the material and behaviour of which it is comprised. The importance of the P100
758 lithic collection – the ‘Pandan’ type assemblage (Mercader et al, 2002) – lies not only in its historical

759 primacy among primate archaeological excavations, but also in the continued value of the Taï Forest
760 material as a touchstone for comparisons with newly discovered hominin sites. Recent developments in
761 the field of primate archaeology and human evolution suggest the need for more nuanced interpretations
762 of chimpanzee percussive technology if we are to use it as an aid in understanding the tool use behaviour
763 of early hominins. Cross-taxa application of analytical methods, as emphasised here, is one of the
764 simplest and clearest ways to improve our confidence in such analogies. Finally, we note that 15 years
765 on from the seminal P100 publication, rigorous reports of additional excavations of chimpanzee sites
766 are very rare. Both for the purpose of understanding how chimpanzee technology evolved, and how our
767 own technology diverged so radically from that of other primates, further exploration of the chimpanzee
768 archaeological record is essential.

769

770 **Acknowledgments**

771 The study was funded by European Research Council Starting Grant #283959 (Primate Archaeology)
772 awarded to M.H. The study of the material was also made possible by European Research Council
773 Starting Grant #283366 (ORACEAF) awarded to Ignacio de la Torre. During writing, T.P was funded
774 by a British Academy Fellowship (Project Number: 542133) and L.V.L was funded by a Leverhulme
775 Early Career Fellowship.

776

777 **Supplementary Online Material**

778 High resolution GIS maps of the Panda 100 excavations are available in the supplementary material.
779 All artefact measurements and technological classifications are available in supplementary material.

780

781 **Bibliography**

- 782 Adams, J., Delgado, S., Dubreuil, L., Hamon, C., Plisson, H., Risch, R., 2006. Functional analysis of
783 macro-lithic artefacts, in: *Functional Analysis of Macro-Lithic Artefacts*.
- 784 Arroyo, A., 2015. *Actividades de Percusion en el Pleistoceno Inferior Estudio comparativo entre los*
785 *objetos de percusión de West Turkana, Olduvai y chimpancés. Universitat Autònoma de*
786 *Barcelona*.
- 787 Arroyo, A., de la Torre, I., 2016. Assessing the function of pounding tools in the Early Stone Age: A
788 microscopic approach to the analysis of percussive artefacts from Beds I and II, Olduvai
789 Gorge (Tanzania). *J. Archaeol. Sci.* 74, 23–34.

790 Arroyo, A., Hirata, S., Matsuzawa, T., de la Torre, I., 2016. Nut Cracking Tools Used by Captive
791 Chimpanzees (*Pan troglodytes*) and Their Comparison with Early Stone Age Percussive
792 Artefacts from Olduvai Gorge. *PLoS One* 11, e0166788.

793 Boesch, C., Boesch, H., 1984a. Mental map in wild chimpanzees: an analysis of hammer transports
794 for nut cracking. *Primates* 25, 160–170.

795 Boesch, C., Boesch, H., 1984b. Possible causes of sex differences in the use of natural hammers by
796 wild chimpanzees. *J. Hum. Evol.* 13, 415–440.

797 Boesch, C., Boesch, H., 1983. Optimization of nut-cracking with natural hammers by wild
798 chimpanzees. *Behaviour* 83, 265–286.

799 Caruana, M.V., Carvalho, S., Braun, D.R., Presnyakova, D., Haslam, M., Archer, W., Bobe, R.,
800 Harris, J.W.K., 2014. Quantifying Traces of Tool Use: A Novel Morphometric Analysis of
801 Damage Patterns on Percussive Tools. *PLoS ONE* 9, e113856.
802 doi:10.1371/journal.pone.0113856

803 Chavaillon, J., 1976. Evidence for the technical practices of Early Pleistocene hominids. Shungura
804 Formations, Lower Omo Valley, Ethiopia. In. (eds) Howell, F. C et al. Earliest man and
805 environments in the Lake Rudolf Basin. Chicago. University of Chicago Press.

806 Chavaillon, J., 1970. Découverte d'un niveau oldowayen dans la basse vallée de l'Omo (Ethiopie).
807 Bull. Société Préhistorique Fr. Comptes Rendus Séances Mens. 67.

808 de la Torre, I., 2004. Omo revisited: evaluating the technological skills of Pliocene Hominids. *Curr.*
809 *Anthropol.* 45, 439–465.

810 de la Torre, I., Benito-Calvo, A., Arroyo, A., Zupancich, A., Proffitt, T., 2013. Experimental protocols
811 for the study of battered stone anvils from Olduvai Gorge (Tanzania). *J. Archaeol. Sci.* 40,
812 313–332.

813 de la Torre, I., Mora, R., 2005. Technological Strategies in the Lower Pleistocene at Olduvai Beds I &
814 II.

815 de la Torre, I., Mora, R., 2004. A technological analysis of non-flaked stone tools in Olduvai Beds I &
816 II. Stressing the relevance of percussion activities in the african Lower Pleistocene, in:
817 Mourre, V., Jarry, M. (Eds.), . Presented at the La percussion directe au percuteur dur et la
818 diversité de ses modalités d'application, PALEO 2009-2010, pp. 13–34.

819 de la Torre, I. 2010. Insights on the Technical Competence of the Early Oldowan. In: Nowell,
820 A and Davidson, I, (eds.) Stone Tools and the Evolution of Human Cognition. pp. 45-65.
821 Univ Pr of Colorado: Boulder.

822 Delagnes, A., Roche, H., 2005. Late Pliocene hominid knapping skills: the case of Lokalalei 2C, West
823 Turkana, Kenya. *J. Hum. Evol.* 48, 435–472.

824 Diez-Martin, F., Sanchez, P., Dominguez-Rodrigo, M., Mabulla, A., Barba, R., 2009. Were Olduvai
825 hominins making butchering tools or battering tools? Analysis of a recently excavated lithic

826 assemblage from BK (Bed II, Olduvai Gorge, Tanzania). *J. Anthropol. Archaeol.* 28, 274–
827 289.

828 Elisabetta, V., Haslam, M., Spagnoletti, N., Fragaszy, D., 2013. Use of stone hammer tools and anvils
829 by bearded capuchin monkeys over time and space: construction of an archeological record of
830 tool use. *J. Archaeol. Sci.* 40, 3222–3232. doi:10.1016/j.jas.2013.03.021

831 Goren-Inbar, N., Sharon, G., Alpersen-Afil, N., Herzlinger, G., 2015. A new type of anvil in the
832 Acheulian of Gesher Benot Ya‘aqov, Israel. *Phil Trans R Soc B* 370, 20140353.
833 doi:10.1098/rstb.2014.0353

834 Goren-Inbar, N., Sharon, G., Melamed, Y., Kislev, M.E., 2002. Nuts, nut cracking, and pitted stones
835 at Gesher Benot Ya‘aqov, Israel. *Proc. Natl. Acad. Sci. U. S. A.* 99, 2455–2460.

836 Harmand, S., Lewis, J.E., Feibel, C.S., Lepre, C.J., Prat, S., Lenoble, A., Boës, X., Quinn, R.L.,
837 Brenet, M., Arroyo, A., Taylor, N., Clément, S., Daver, G., Brugal, J.-P., Leakey, L.,
838 Mortlock, R.A., Wright, J.D., Lokorodi, S., Kirwa, C., Kent, D.V., Roche, H., 2015. 3.3-
839 million-year-old stone tools from Lomekwi 3, West Turkana, Kenya. *Nature* 521, 310–315.
840 doi:10.1038/nature14464

841 Haslam, M., Hernandez-Aguilar, R.A., Proffitt, T., Arroyo, A., Falótico, T., Fragaszy, D., Gumert,
842 M., Harris, J.W., Huffman, M.A., Kalan, A.K., 2017. Primate archaeology evolves. *Nature*
843 *Ecology & Evolution* 1, 1431.

844 Haslam, M., 2012. Towards a prehistory of primates. *Antiquity* 86, 299–315.

845 Haslam, M., Hernandez-Aguilar, A., Ling, V., Carvalho, S., de la Torre, I., DeStefano, A., Du, A.,
846 Hardy, B., Harris, J., Marchant, L., Matsuzawa, T., McGrew, W.C., Mercader, J., Mora, R.,
847 Petraglia, M., Roche, H., Visalberghi, E., Warren, R., 2009. Primate archaeology. *Nature* 460,
848 339–344.

849 Haslam, M., Luncz, L., Pascual-Garrido, A., Falótico, T., Malaivijitnond, S., Gumert, M., 2016a.
850 Archaeological excavation of wild macaque stone tools. *J. Hum. Evol.*
851 doi:10.1016/j.jhevol.2016.05.002

852 Haslam, M., Luncz, L.V., Staff, R.A., Bradshaw, F., Ottoni, E.B., Falótico, T., 2016b. Pre-Columbian
853 monkey tools. *Curr. Biol.* 26, R521–R522.

854 Isaac, G.L., 1976. Plio-Pleistocene artifact assemblages from east Rudolf, Kenya, in: *Early Man and*
855 *Environments in the Lake Rudolf Basin: Stratigraphy, Paleoecology and Evolution.*
856 University of Chicago Press, Chicago, pp. 552–564.

857 Kortlandt, A., 1986. The use of stone tools by wild-living chimpanzees and earliest hominids. *J. Hum.*
858 *Evol.* 15, 77–132.

859 Leakey, M.D., 1971. *Olduvai Gorge, Vol. 3. Excavations in Beds I and II, 1960-1963.* Cambridge
860 University Press, Cambridge.

- 861 Lewis, J.E., Harmand, S., 2016. An earlier origin for stone tool making: implications for cognitive
862 evolution and the transition to Homo. *Phil Trans R Soc B* 371, 20150233.
863 doi:10.1098/rstb.2015.0233
- 864 Luncz, L.V., Proffitt, T., Kulik, L., Haslam, M., Wittig, R.M., 2016. Distance-decay effect in stone
865 tool transport by wild chimpanzees. *Proc. R. Soc. B Biol. Sci.*
- 866 Marchant, L.F., McGrew, W.C., 2005. Percussive technology: Chimpanzee baobab smashing and the
867 evolutionary modelling of hominin knapping, in: Roux, V., Brill, B. (Eds.), *Stone Knapping,
868 the Necessary Conditions for a Uniquely Hominin Behaviour*. McDonald Institute for
869 Archaeological Research, Cambridge, pp. 341–350.
- 870 McGrew, W.C., 1992. *Chimpanzee material culture: implications for human evolution*. Cambridge
871 University Press, Cambridge.
- 872 McNabb, J., 1998. On the move. Time, averaging and resource transport in the Oldowan.
- 873 Mercader, J., Barton, H., Gillespie, J., Harris, J., Kuhn, S., Tyler, R., Boesch, C., 2007. 4,300-year-old
874 chimpanzee sites and the origins of percussive stone technology. *Proc. Natl. Acad. Sci. U. S.*
875 *A.* 104, 3043–3048.
- 876 Mercader, J., Panger, M.A., Boesch, C., 2002. Excavation of a chimpanzee stone tool site in the
877 african rainforest. *Science* 296, 1452–1455.
- 878 Merrick, H.V., De Heinzelin, J., Haesaerts, P., Howell, F.C., 1973. Archaeological Occurrences of
879 Early Pleistocene Age from the Shungura Formation, Lower Omo Valley, Ethiopia. *Nature*
880 242, 572–575. doi:10.1038/242572a0
- 881 Merrick, H.V., Merrick, J.P., 1976. Archaeological occurrences of Earlier Pleistocene Age from the
882 Shungura Formation, in: Coppens, Y., Howe, F.C., Isaac, G.L., Leakey, R.E. (Eds.), *Earliest
883 Man and Environment in the Lake Rudolf Basin*. University of Chicago Press, Chicago, pp.
884 574–584.
- 885 Mora, R., de la Torre, I., 2005. Percussion tools in Olduvai Beds I and II (Tanzania): Implications for
886 early human activities. *J. Anthropol. Archaeol.* 24, 179–192.
- 887 Panger, M.A., Brooks, A.S., Richmond, B.G., Wood, B., 2003. Older than the Oldowan? Rethinking
888 the emergence of hominin tool use. *Evol. Anthropol. Issues News Rev.* 11, 235–245.
889 doi:10.1002/evan.10094
- 890 Pelegrin, J., 2005. Remarks about archaeological techniques and methods of knapping: Elements of a
891 cognitive approach to stone knapping., in: Roux, V., Brill, B. (Eds.), *Stone Knapping: The
892 Necessary Conditions for a Uniquely Hominid Behaviour*. McDonald Institute Monograph
893 Series, Cambridge. McDonald Institute monograph series, Cambridge, pp. 23–33.
- 894 Proffitt, T., Luncz, L.V., Falótico, T., Ottoni, E.B., de la Torre, I., Haslam, M., 2016. Wild monkeys
895 flake stone tools. *Nature*.
- 896 Schick, K., Toth, N., 2006. An overview of the Oldowan Industrial Complex: the sites and the nature
897 of their evidence. *Oldowan Case Stud. Earliest Stone Age* 3–42.

- 898 Semaw, S., 2000. The World's Oldest Stone Artefacts from Gona, Ethiopia: Their Implications for
899 Understanding Stone Technology and Patterns of Human Evolution Between 2.6 - 1.5 Million
900 Years Ago. *J. Archaeol. Science* 27, 1197–1214.
- 901 Semaw, S., Renne, P., Harris, J.W., Feibel, C.S., Bernor, R.L., Fesseha, N., Mowbray, K., 1997. 2.5-
902 million-year-old stone tools from Gona, Ethiopia. *Nature* 385, 333–336.
- 903 Stout, D., Semaw, S., Rogers, M.J., Cauche, D., 2010. Technological variation in the earliest Oldowan
904 from Gona, Afar, Ethiopia. *J. Hum. Evol.* 58, 474–491.
- 905 Turq, A., 1992. Le Paleolithique inferieur et moyen les vallees de la Dordogne et due Lot. Universite
906 de Bordeaux I.
- 907 Visalberghi, E., Spagnoletti, N., Ramos da Silva, E.D., Andrade, F.R.D., Ottoni, E., Izar, P., Fragaszy,
908 D., 2009. Distribution of potential suitable hammers and transport of hammer tools and nuts
909 by wild capuchin monkeys. *Primates* 50, 95–104. doi:10.1007/s10329-008-0127-9

910

911

912 **List of Tables**

913 Table 1: Calibrated radiocarbon ages from the Panda 100 site (Mercader et al., 2007), calibrated using
914 OxCal 4.2 and the IntCal13 curve

915

916 Table 2: Absolute and relative frequency of technological artefact types for each raw material at
917 Panda 100

918

919 Table 3: Dimensional data for each percussive technological category at Panda 100

920

921 Table 4: All refits identified in the current study of the Panda 100 lithic assemblage. * No direct
922 measurement possible for entire refit sequence, distance was estimated based on grid reference. ¹ No
923 direct measurement possible for a single piece in refit set, distance was estimated based on grid
924 reference.

925

926 Table 5: Percussive damage identified on lithic artefacts from P100

927

928 **List of Figures**

929 Figure 1: (A) Location map of Panda 100 (P100) site. (B) Excavation and refit map of P100 lithic
930 assemblage (adapted from (Mercader et al., 2002)

931

932

933 Figure 2: Examples of detached percussive products from lithic hammerstones at P100. A) Granitoid
934 and diorite edge pieces (Group 1.1). B) Granitoid and diorite corner fragments (Group 1.2). C)
935 Examples of granitoid and laterite small debris (<20mm) (Group 5) (Scale = 5cm).

936

937 Figure 3: Examples of detached percussive artefacts from lithic hammerstones at P100. A) Detached
938 diorite conchoidal flake (Group 2.3). B) Detached diorite typical hammerstone flakes (Group 3).
939 (Scale = 5cm)

940

941 Figure 4: Refit Sets 1 and 2 from Panda 100. A) Refit Set 1: Two laterite angular chunks. B) Refit Set
942 2: Distally fractured, detached corner fragment of a diorite hammerstone (Scale = 5cm)

943

944 Figure 5: Refit Sets 3 and 4 from Panda 100. A) Refit set 3: Four granitoid fragments, two edge
945 fragments and two corner fragments. B) Refit Set 4: Two granitoid fragments representing a corner
946 region of a hammerstone (Scale = 5cm)

947

948 Figure 6: Refit Set 5, 6 and 7 from Panda 100. A) Refit Set 5: Two angular chunks representing the
949 edge of a granitoid hammerstone. B) Refit Set 6: Two corner fragments and one angular chunk
950 representing a corner detachment of a granitoid hammer. C) Refit Set 7: Corner refit of a tabular
951 granitoid hammerstone consisting of three corner fragments and one edge fragment. (Scale = 5cm)

952

953 Figure 7: Refit Sets 8 and 9 from Panda 100. A) Refit Set 8: Edge fragment of a granitoid
954 hammerstone consisting of one corner fragment and one edge fragment. B) Refit Set 9: Minor
955 fragmentation of a laterite cobble. (Scale = 5cm)

956

957 Figure 8: Refit Sets 10, 11, and 12 from Panda 100. A) Refit Set 10: Five granitoid fragments (three
958 corner fragments, two angular chunks) representing an extensive fragmentation of a large
959 hammerstone. B) Refit Set 12: Five granitoid fragments (two edge fragments, three angular chunks /
960 fragments) of a larger hammerstone corner region. C) Refit Set 11: Edge fragment of a granitoid
961 hammerstone consisting of one angular chunk and one edge fragment. (Scale = 5cm)

962

963 Figure 9: Spatial map of Panda 100 excavations highlighting all refit sets identified in this study

964

965 Figure 10: All mapped artefacts separated by spit with corresponding refit sets for each anvil location

966

967 Figure 11: Microscopic damage of percussive artefacts at Panda 100. A) Granitoid corner fragment
968 (Group 1.2) with clear percussive damage. 1 and 2. Cortical, undamaged areas, showing intact quartz
969 crystals and flat smooth surface (scale = 500µm and 1000µm). 3 and 4. Impact point showing

970 significant crushing and development of small steps along with detachment of quartz crystals (scale =
971 500µm and 1000µm). B) Granitoid edge fragment (Group 1.1). 1. Undamaged cortical surface (scale
972 = 500µm). 2, 3 and 4. V-shaped impact points along the edge and interior of the percussive surface
973 (scale 3000µm, 3000µm and 500µm).

974

975 Figure 12: Microscopic damage of percussive artefacts at Panda 100. A) Granitoid corner fragment
976 with clear percussive damage. 1. Cortical, undamaged surface (scale = 500µm). 2. V-shaped impact
977 point (scale 3000µm). 3. Crushing and step fractures associated with impact point (scale = 3000µm).
978 4. Impact point showing significant crushing of quartz crystals and matrix (scale = 1000µm). B)
979 Diorite corner fragment with possible pitted surface. 1 and 2. Cortical, undamaged surfaces preserving
980 intact crystals and matrix. 3 and 4. Undamaged surface from within the pitted surface, showing intact
981 crystals and matrix (scale = 2000µm).

982

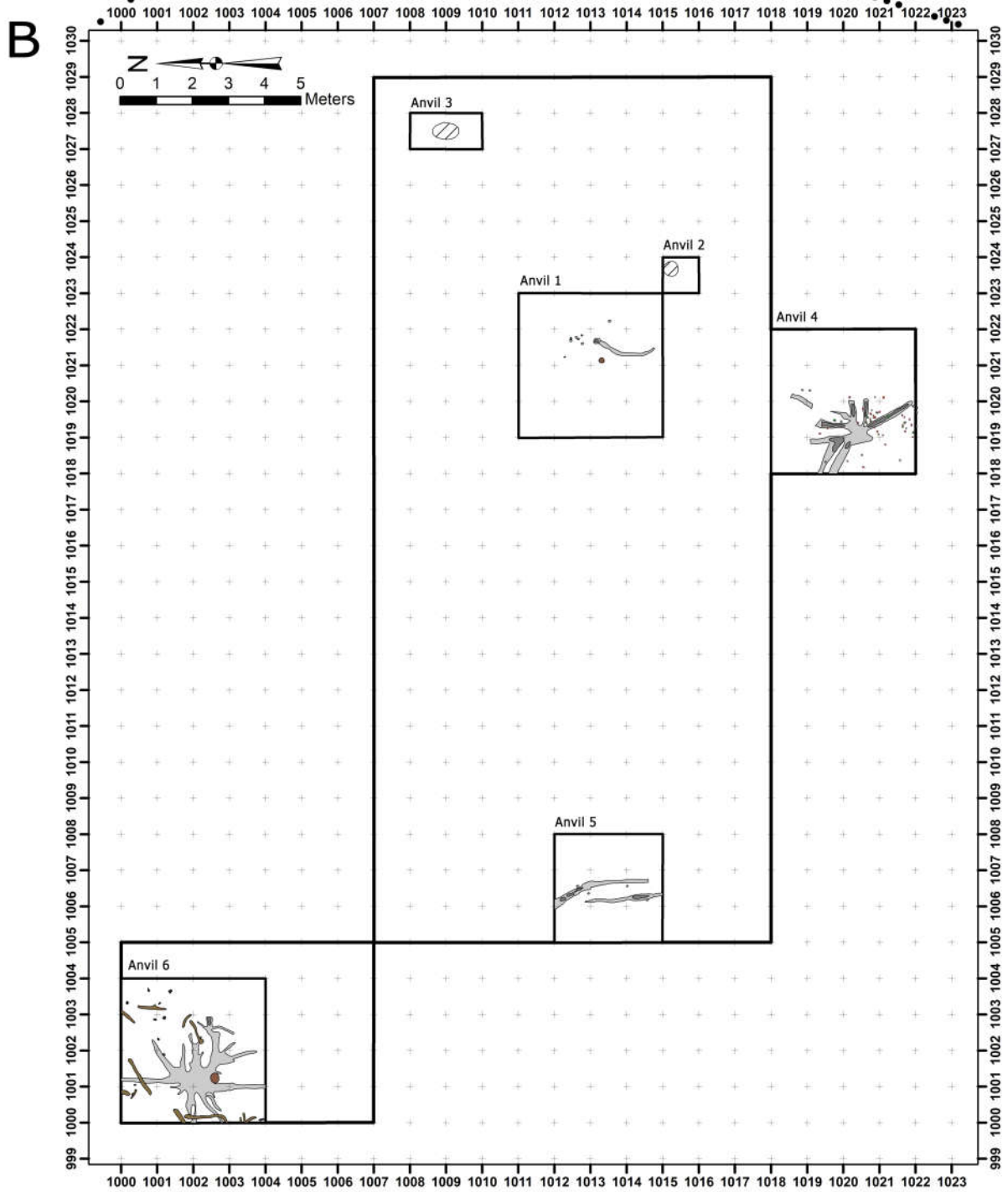
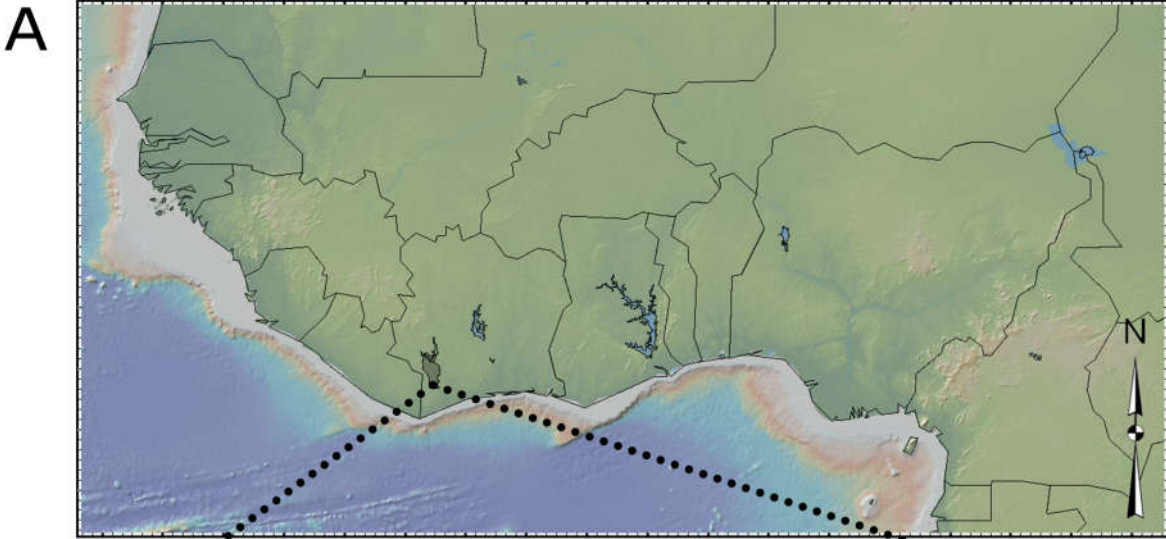
983 Figure 13: Density map of all artefacts at Panda 100 at each anvil location

984

985

986

987

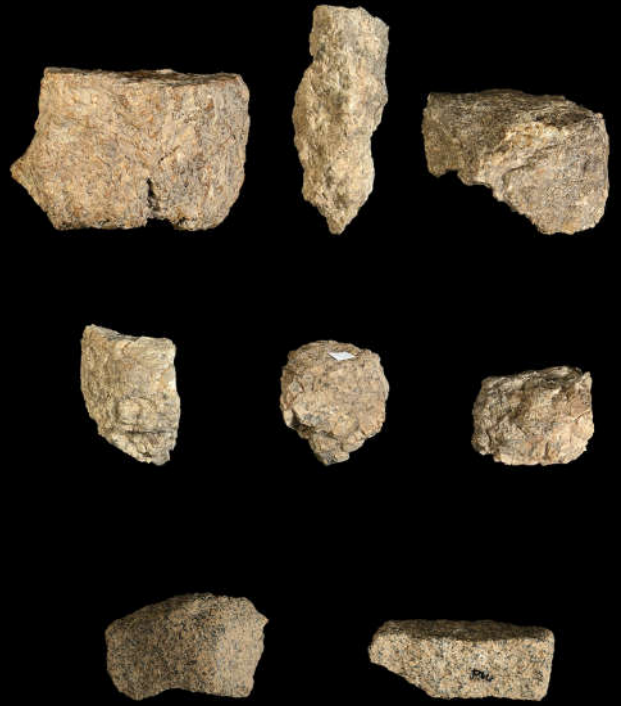


A



Group 1.1 

B



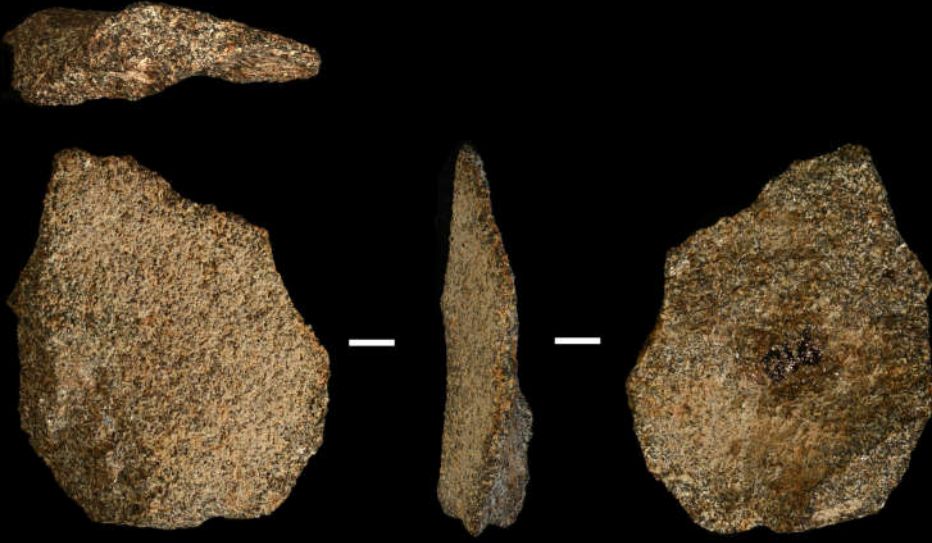
Group 1.2 

C



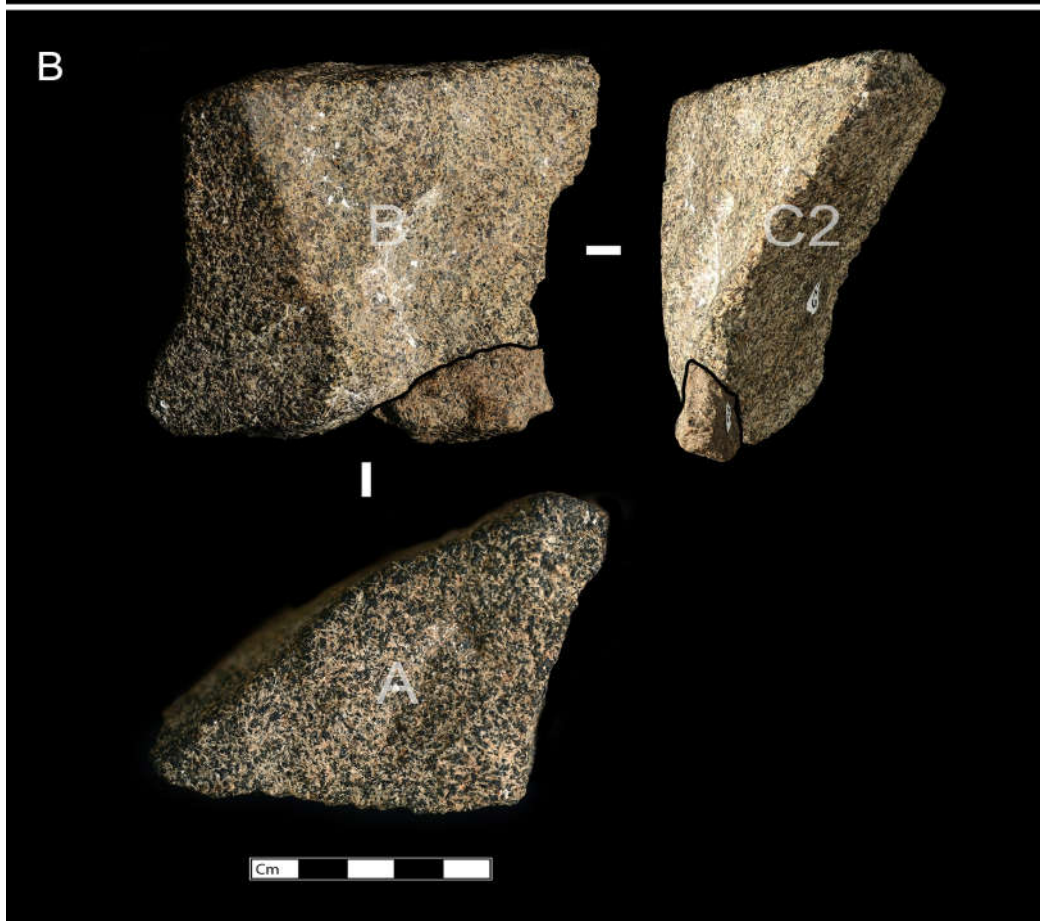
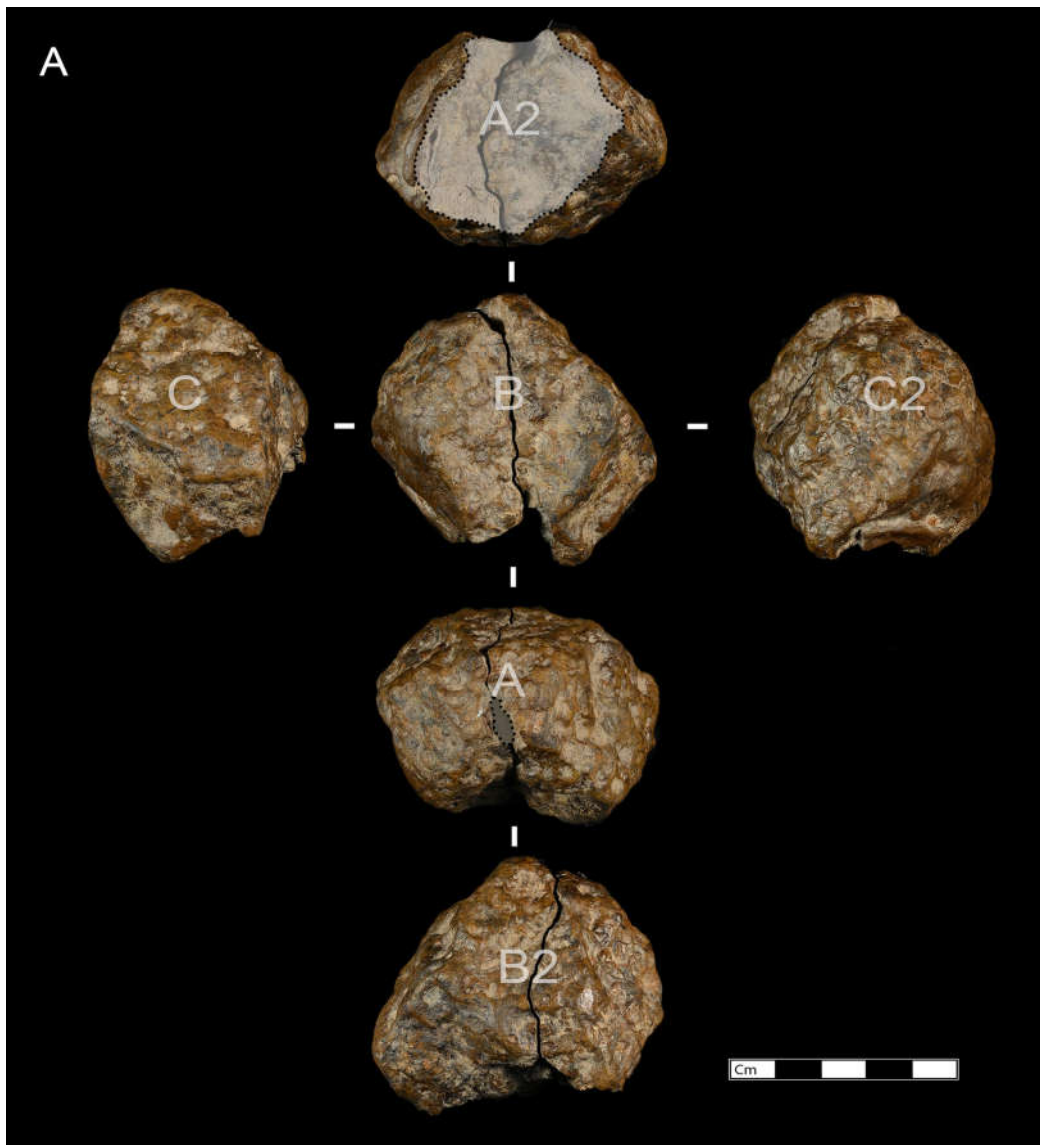
Group 5 

A

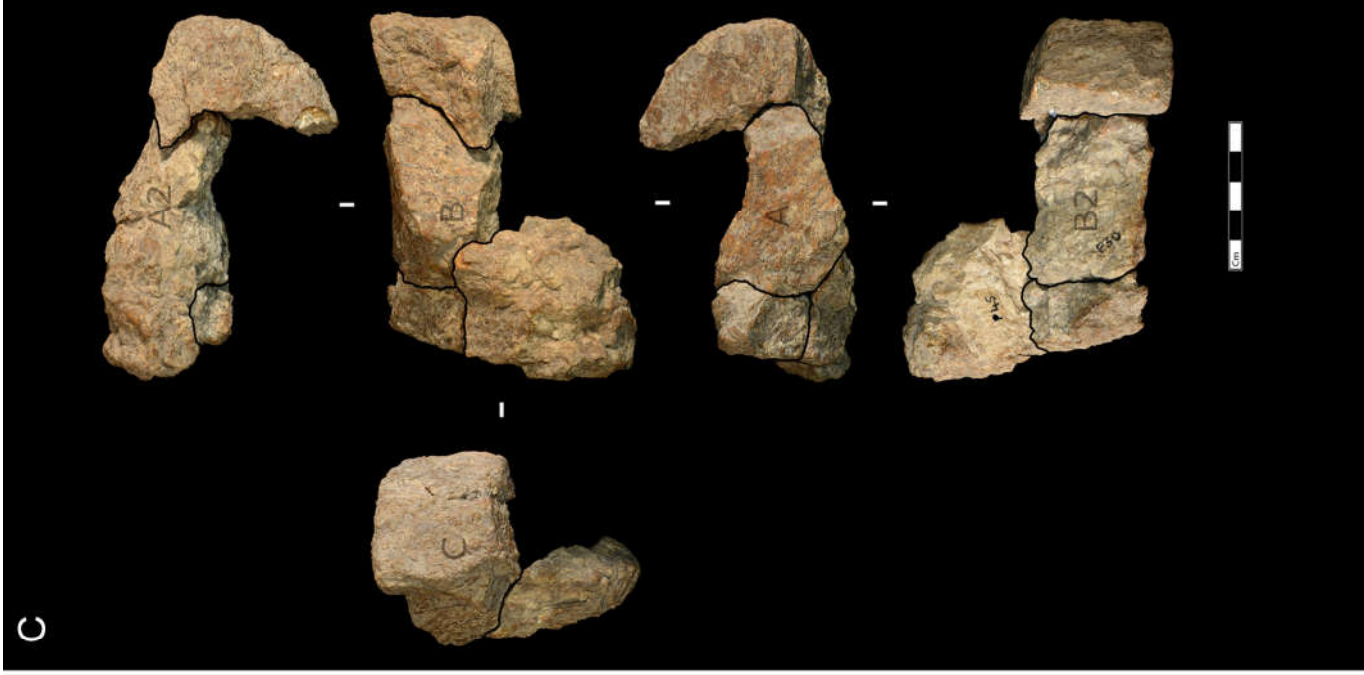
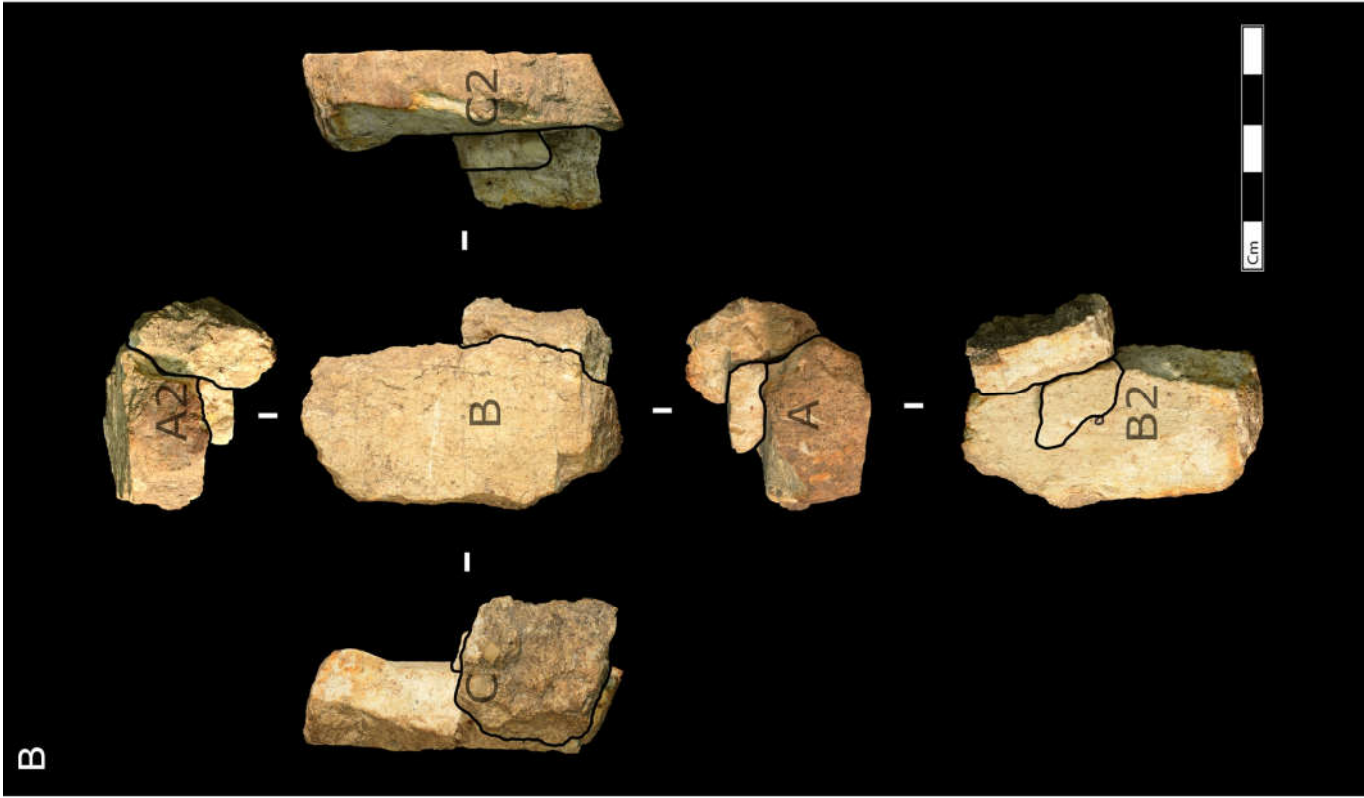
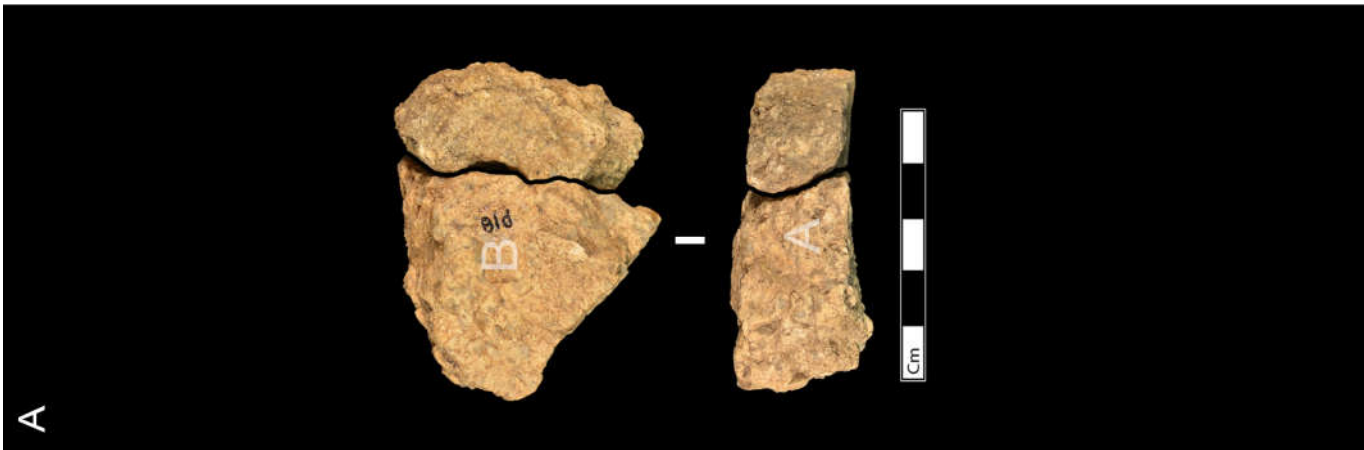


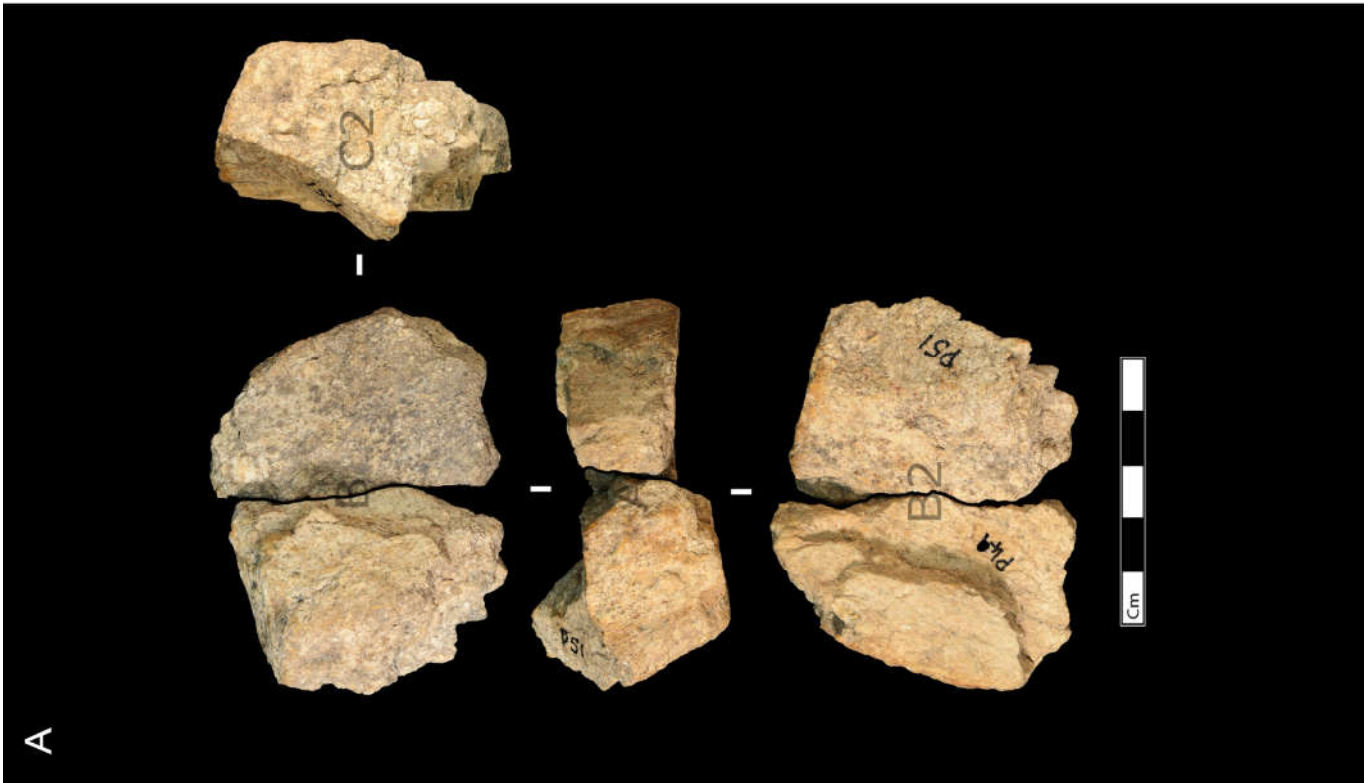
B

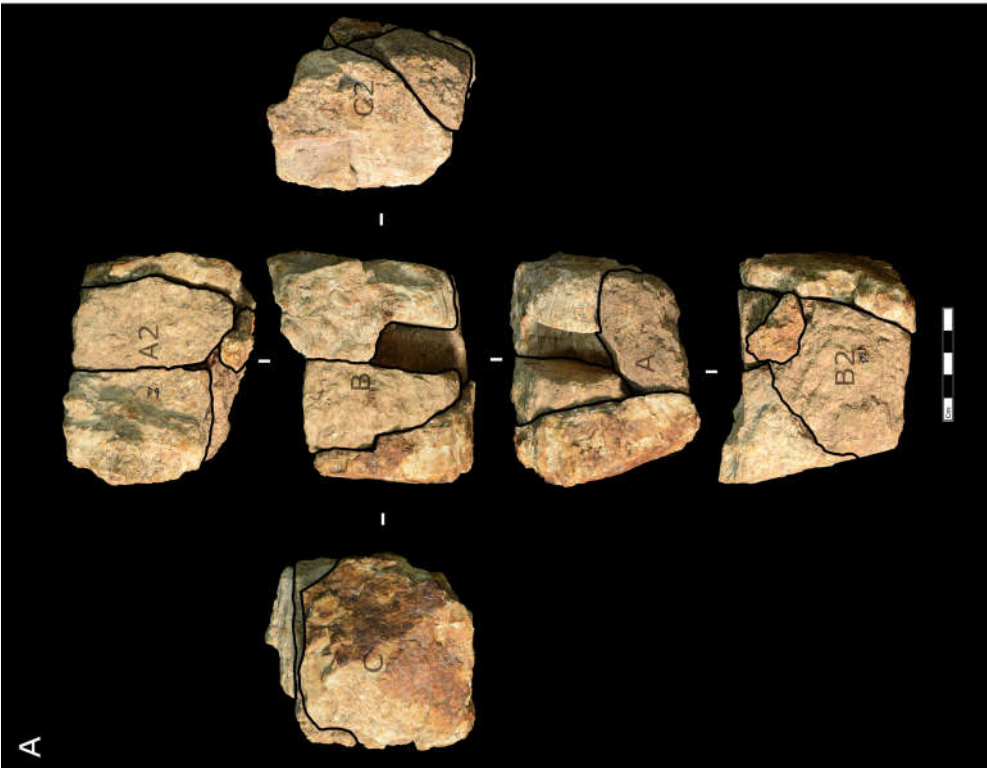
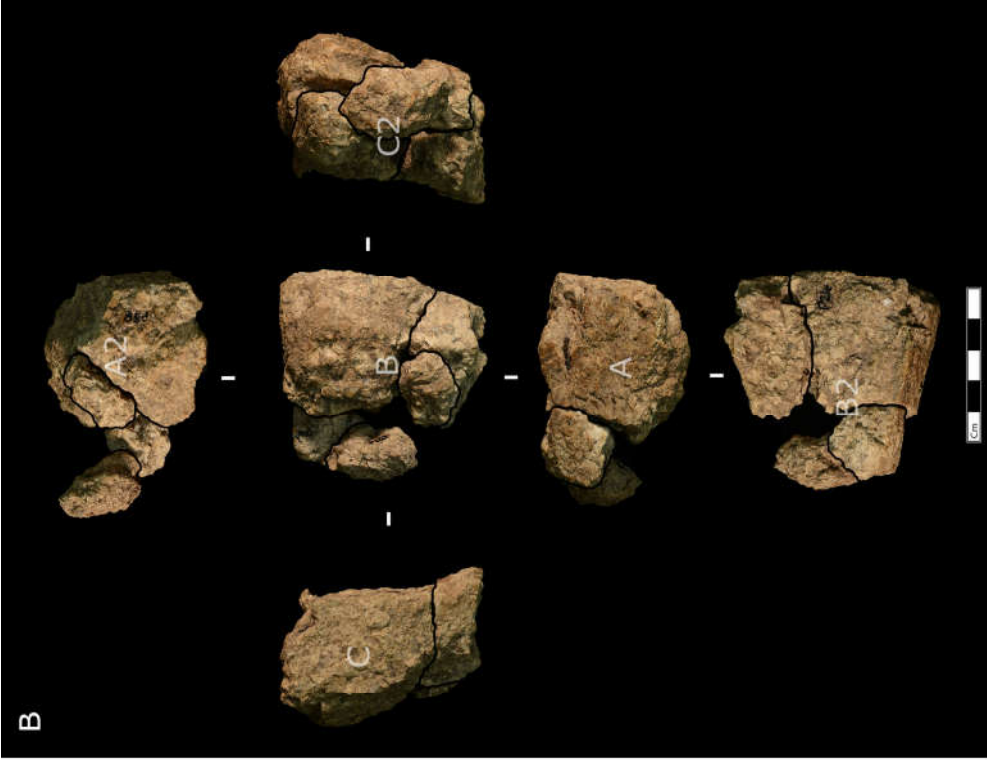


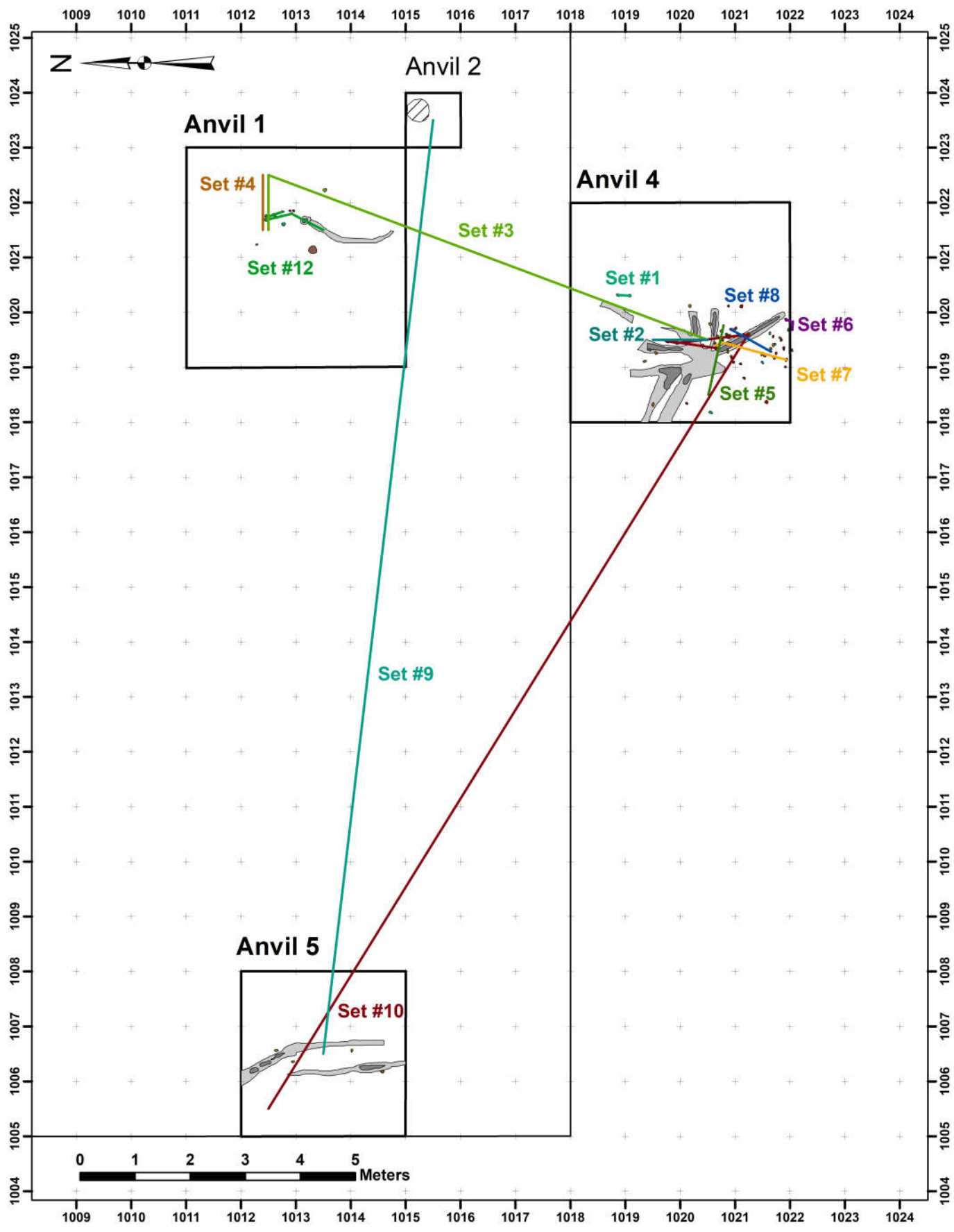


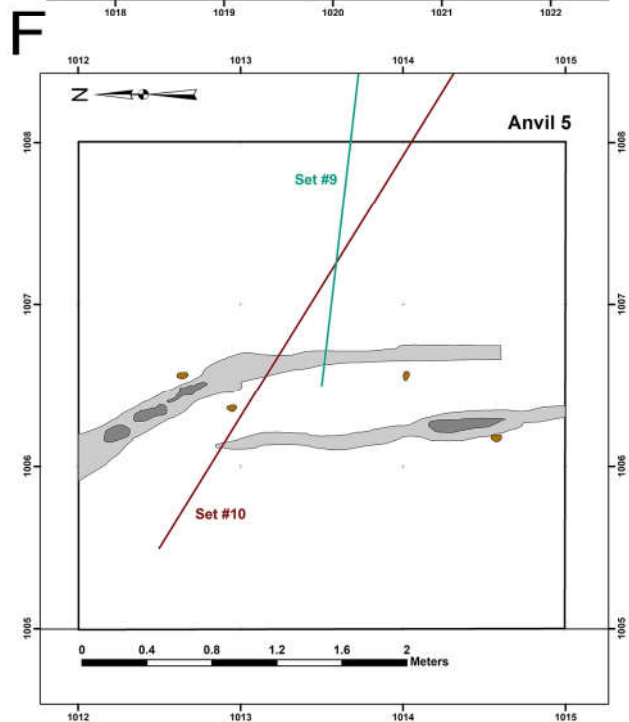
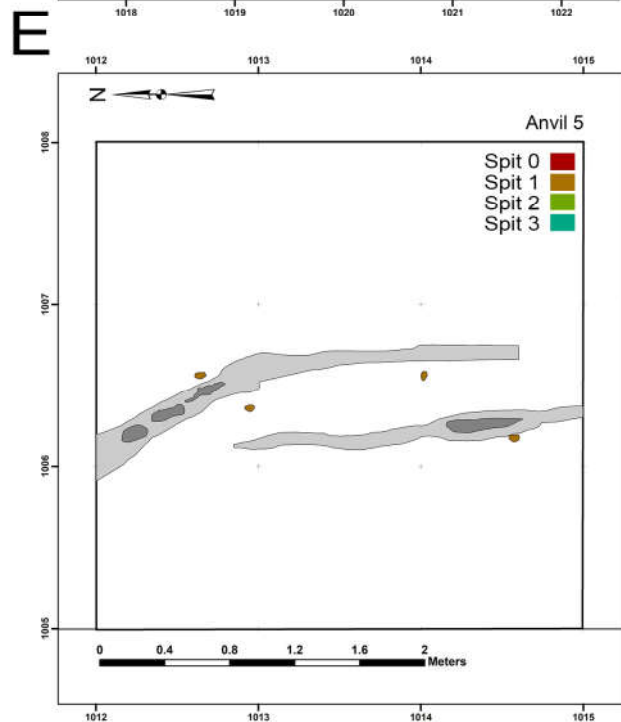
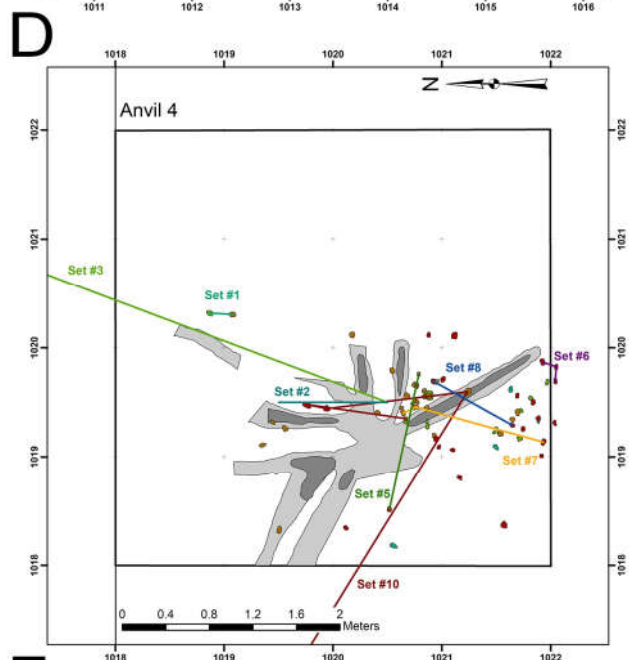
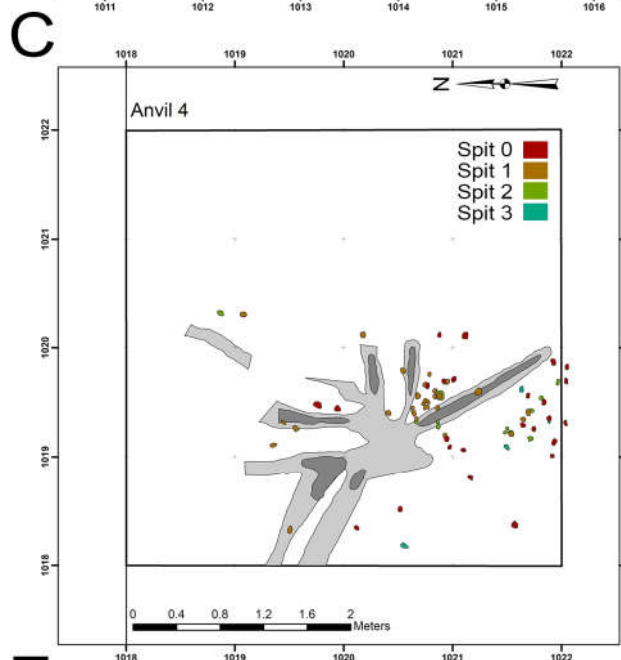
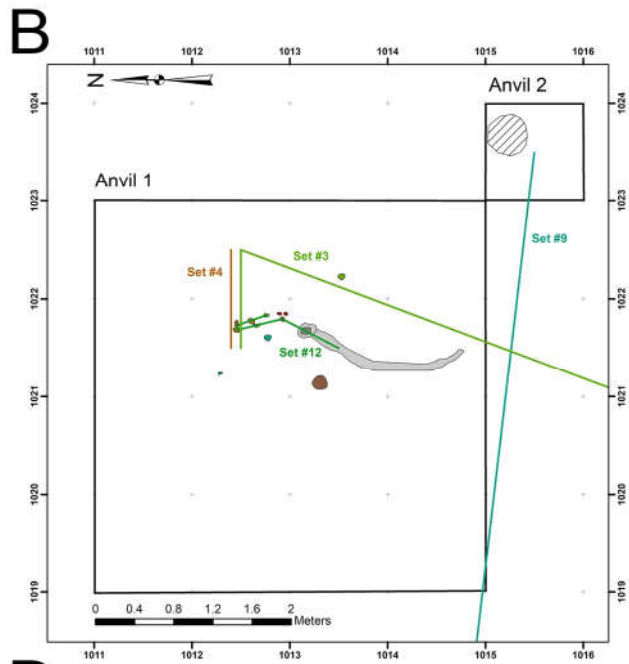
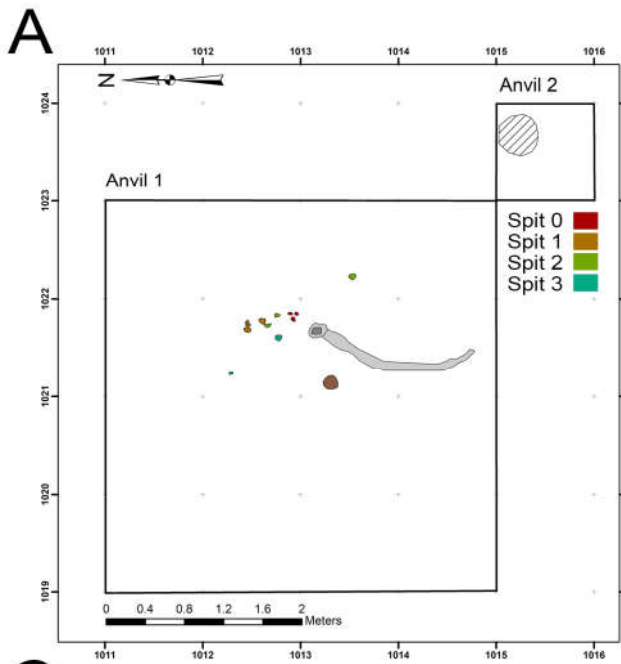




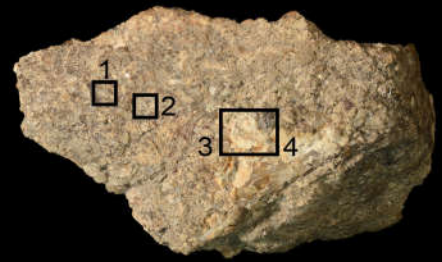
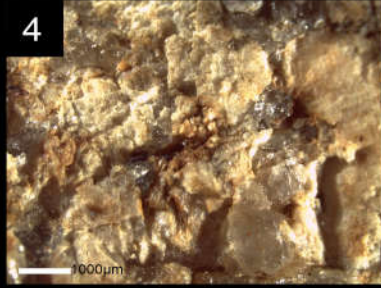
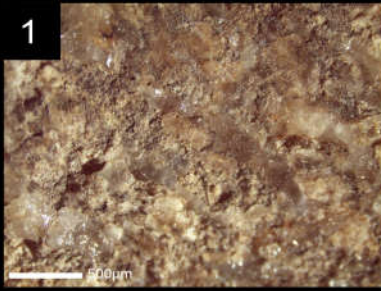




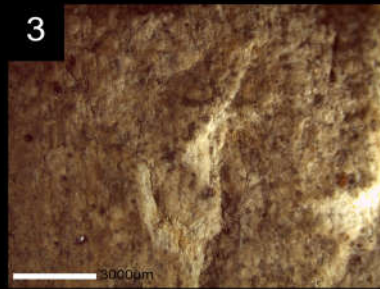
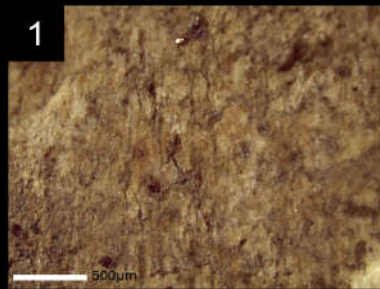
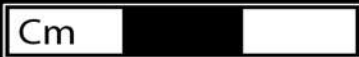
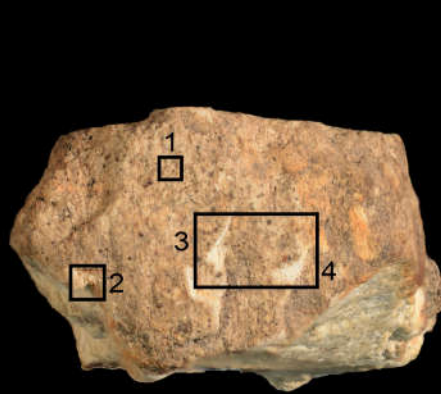




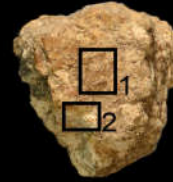
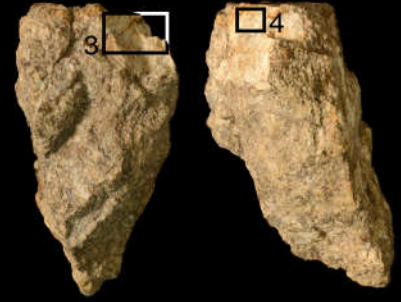
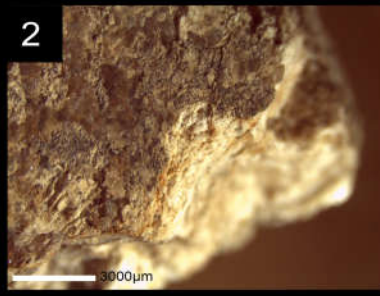
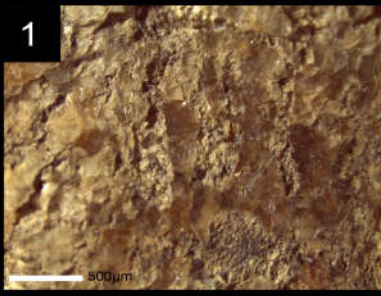
A



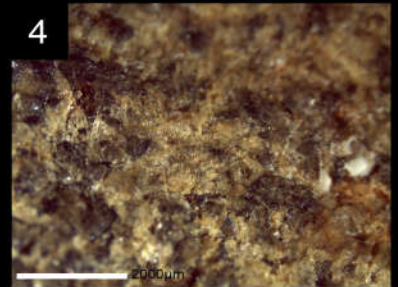
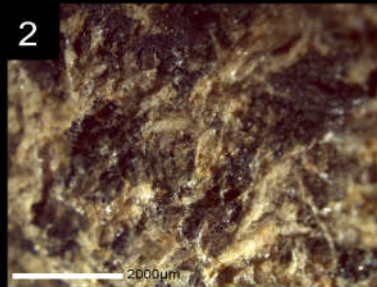
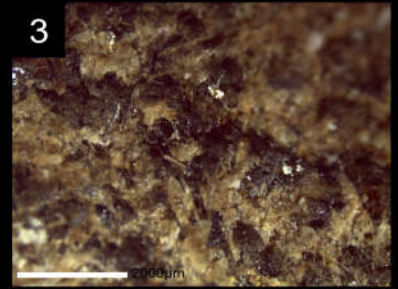
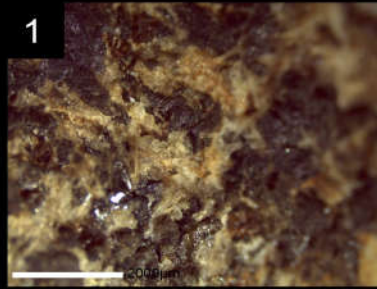
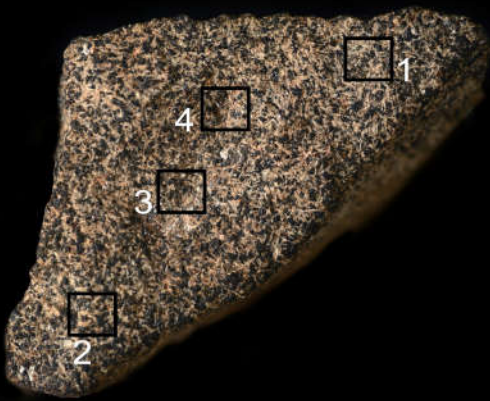
B

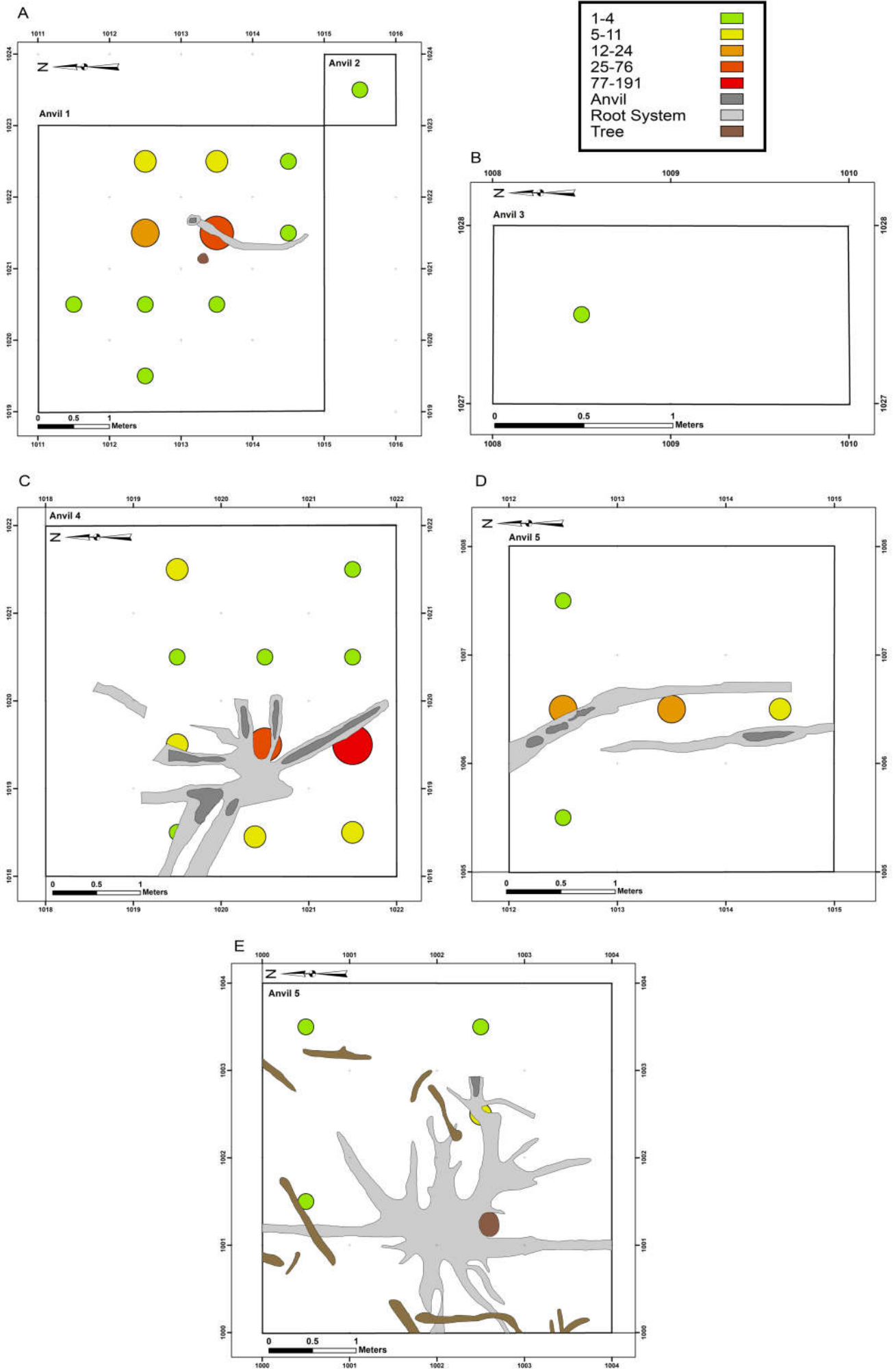


A



B





Supplementary Material 2

Panda 100 Refit Analyses

Refit Set 1:

Refit Set 1 (Figure 4) is comprised of two angular chunks from a small laterite cobble, one of which was originally reported as a hammer fragment (Mercader et al., 2002, Fig. 2A). Both pieces were recovered from the same meter square at Anvil 4 with a horizontal distance of 0.21 meters, and are derived from spits 1 and 2 suggesting a degree of vertical movement (Table 4).

This cobble fractured into four separate pieces, two of which are represented in the refit and two by unfitted fractures. No macroscopic evidence of percussive damage associated with the fracturing of the cobble is identifiable. However, a small area of wedge initiated fracturing on a convex protrusion on Plane A, which spans both refitted pieces, may be a result of percussive impact. The cortex of the cobble is highly weathered and smooth, with no evidence of percussive related pitting or crushing.

Although not fully refitted, the maximum dimensions of the cobble are apparent (60.5 x 56.9 x 45.5mm). Ordinarily chimpanzee hammerstones used for *Panda* nut processing are considerably larger, possessing a mean weight of up to 17 kg (Boesch and Boesch, 1984a; Luncz et al., 2016). Because of its diminutive size, the cobble represented in Refit Set 1 is therefore unlikely to have been used as a *Panda* nut hammerstone. This finding does not preclude its use for processing other, more easily cracked nut species such as *C. edulis*, provided those activities left little surficial evidence of percussive damage, however P100 is an isolated Panda tree with no *C. edulis* sources close by. Conversely, it is known that infant nut cracking experimentation involves the use of smaller sized hammerstones.

Refit Set 2

Refit Set 2 (Figure 4) is the only refit identified in the original excavation report (Mercader et al., 2002, Fig 2E). This set represents a distally fractured, detached corner fragment of a diorite hammerstone. It includes a single corner fragment and a single edge fragment. There is little evidence of percussive damage observable on either piece, however, the clean nature of the ventral fracture suggests that this piece was detached through a relatively high degree of force.

The refitted fragments are derived from adjacent metre squares within the vicinity of Anvil 4, representing between 1-2 m of horizontal movement. A degree of vertical movement is also represented, between spits 0 and 1 (Table 4). As the smaller distal piece does not possess any identifiable impact point and is clearly derived from the same detachment event as the larger corner fragment, any spatial patterning between the two should not be associated with chimpanzee movement.

Refit Set 2 provides insight into the original morphology of the diorite hammerstones used for *Panda* nut processing at P100. The refit preserves portions of Planes A, B and the opposed Plane A2, indicating a tabular morphology of the original hammerstone with a minimum thickness of 73.1 mm. The active plane possessed a flat morphology, as indicated by the preserved platform on the larger of the two refitted pieces. No previous detachments are present on the dorsal surface of this corner fragment, indicating that this fragment was detached from an unbroken surface.

Refit Set 3

Refit Set 3 (Figure 5) consists of four granitoid fragments: two edge (Group 1.1) and two corner fragments (Group 1.2). Combined, this refit set represents the fragmentation of the corner and associated edge region of a hammerstone. A series of discreet impact points in association with small areas of crushing located on a single plane of the reconstructed set indicates the location of the active percussive plane (Plane A), as well as suggesting the direction of the detachments.

At least two separate fragmentation events are represented by this refit. The first occurred within close proximity to Anvil 4, and the second at Anvil 1, a horizontal transport of 9.54 m and a vertical movement between spits 1-2 (Table 4). The first fragmentation stage included the detachment of a singular edge piece and associated corner fragment. At some point following these detachments the hammerstone was transported from Anvil 4 to Anvil 1, where a second sequence of fracturing involved one edge fragment and one corner fragment being detached from the same corner area as the initial fragmentation. The close proximity of the two sequences of detachments might be either due to an internal weakness within this area of the hammer, as seen in the presence of a significant fracture plane on the ventral surfaces of all pieces within the refit, or it may have occurred due to continuing use of the same active plane.

The morphology of the original hammerstone can be partially reconstructed from the completed refit set. Plane A of the refit is a cortical surface, with relatively rounded margins and a slightly weathered surface, while Plane A2 possess the flat morphology of a fracture plane of the original granitoid block. The presence of percussive impacts on the cortical Plane A suggests that this surface was the active percussive plane, and that Plane A2 represents the outer surface of the original hammerstone at the point of this fragmentation sequence. The minimum length or width of the original hammerstone cannot be determined, but the minimum thickness was around 35 mm.

Refit Set 4

Refit Set 4 (Figure 5) is a corner region of a granitoid hammerstone, consisting of one corner and one edge fragment. Both pieces were recovered from the vicinity of Anvil 1, from neighbouring meter squares, representing between 1-2 m of horizontal movement within a single spit (Table 4).

Similar to other refitted sequences, Refit Set 4 records the detachment of the edge of a hammerstone as well as detachment of the intersecting edge of Plane A and B. Initially a small corner area of the hammerstone was detached, followed by a larger edge piece. The superimposed fragmentation of these edge margins rapidly reduces the dimensions of the hammerstone. The direction in which the fracture occurred, seen in the step termination of the corner fragment, makes it likely that a previously fractured, non-cortical surface (Plane A) was the active percussive plane at the time of breakage, although the cortical Plane C may also have been the active plane resulting in this detachment.

Refit Set 5

Refit Set 5 (Figure 6) is comprised of two angular chunks (Group 2.2) which refit along an internal fracture plane. No percussive impact points, nor the active percussive plane from which these fragments originated, are identifiable. The pieces were recovered from neighbouring squares at Anvil 4 representing 1.27m of horizontal movement between spits 0-1 (Table 4).

Refit Set 6

Refit Set 6 (Figure 6) records the invasive detachment of a corner region of a granitoid hammerstone, caused by the hammerstone splitting along an internal fracture plane. It is comprised of three tabular fragments, two corner fragments and a single angular chunk. All refitted pieces were located in a single metre square at Anvil 4, representing a horizontal movement of 0.26m within a single spit (Table 4).

The presence of significant internal fracture planes within the P100 granitoid hammerstones has contributed to their increased rate of fragmentation, and would have resulted in significant mass loss during percussive activities. The pieces in Refit Set 6 fragmented through a forceful wedging initiation that detached a corner region of a tabular hammerstone in its entirety. The sequence of fragmentation can be inferred by the presence of macroscopically visible impact points on the cortical platform of the edge fragment, suggesting the initial detachment of an elongated corner fragment that subsequently broke into at least two separate pieces. This event was followed by the detachment of an edge fragment as well as at least one internal angular fragment. These detachments spanned the entire thickness of the hammerstone. The cortical outer surfaces are preserved at both distal and proximal ends of the refit and can be used to estimate a minimum thickness of the original hammerstone of 62.4 mm.

Refit Set 7

Refit Set 7 (Figure 6) comes from a roughly tabular, granitoid hammerstone. It includes three corner fragments and one edge fragment. All pieces are derived from two neighbouring metre squares at Anvil 4 representing a horizontal movement of 1.34m between spits 0 – 1 (Table 4).

Protruding angular regions of the hammerstone, located around its edges, readily broke during use. This refit represents a minimum of two separate impacts, the first detaching a large corner fragment. This piece overlays, and therefore precedes, the later breakage of a group of three fragments that may have been detached at the same time due to a single percussive impact. This fragmentation occurred with no rotation of the hammerstone, from the same active percussive plane (Plane A), and it detached a substantial volume of the corner and edge of the hammerstone as well as reaching the opposite plane.

A central void, where the remaining volume of the hammerstone would be located, could not be refitted and in all likelihood indicates that the remainder of the hammerstone was removed by chimpanzees from the anvil location after the refit set was detached. The refit preserves very little identifiable percussive damage on its cortical surfaces.

Refit Set 8

Refit Set 8 (Figure 7) documents the fragmentation of the edge of a tabular granitoid hammerstone and is comprised of two pieces: a corner fragment and a single edge fragment. Both pieces are found in neighbouring meter squares at Anvil 4 representing a horizontal movement of 0.83m within a single spit. Fragmentation occurred along a pre-existing internal fracture plane, which detached the corner of the hammerstone. These flat internal fracture planes have been identified in a number of fragmented pieces, and result in the fragments possessing a broadly tabular morphology. Both horizontal planes (A and A2) are preserved in this refit set, indicating a minimum thickness of 50 mm of the hammerstone at the breakage point.

Refit Set 9

Refit Set 9 (Figure 7) represents minor fragmentation of a laterite cobble, consisting of one edge fragment and one angular chunk. This refit provides a case of inter-anvil transportation, between Anvil 2 and Anvil 5, which is a horizontal transport distance of 17.12 m within a single spit (Table 4). The direction of travel is unknown as it is not possible to ascertain the order of fragmentation. No clear percussive damage is evident on either conjoining piece, however, its percussive origin is confirmed by the significant conjoining distance. The angular chunk represented in this refit, was used in the initial report as an example of a laterite flake (Mercader et al., 2002, Fig 3I). Refit Set 9, however, allows a clearer understanding of process behind the detachment of this chunk, which bears no evidence of flake

detachment and does not have the morphological characteristics of a detached flake nor is it detached from a position of the cobble which would have produced a flake detachment.

Refit Set 10

Refit Set 10 (Figure 8) is one of the most extensive refits at P100, and records significant fragmentation of a granitoid percussive hammerstone. It is comprised of five fragments: three corner fragments (Group 1.2), one interior angular chunk (Group 2.2) and one indeterminate angular chunk (Group 4).

This refit set represents the transport of a hammerstone between Anvil 4 and Anvil 5, totalling a distance of 16.59 m between two spits (Table 4). The fragmentation sequence can be determined based on the spatial mapping of this refit set. A single small cortical angular chunk was detached spontaneously from the exterior of Plane B2 at Anvil 5. This was followed by a transportation of the hammerstone to Anvil 4, where the majority of the fragmentation occurred. Plane A was used as the active percussion plane, shown by an area of crushing and slight pitting. As no other areas of percussive damage are identified this fragmentation appears to result from a single strike in combination with a number of internal fracture planes.

This refit set also provides a wider context to the illustrated pieces identified in the original P100 publication (Mercader et al., 2002, Fig 3A), allowing for a refinement of its classification. In this case, a large corner fragment, originally described as a partially cortical flake with evidence of previous removals is instead a product of an internal fracture plane, with no previous dorsal surface extractions, no impact point or knapping platform, no bulb of percussion and no evidence of previous removals, instead possessing a distinct patina. This piece instead is a fine example of a corner fragment, similar in many respects to those identified in previous studies at early hominin archaeological sites (De la Torre and Mora, 2005).

Refit Set 11

Refit Set 11 (Figure 8) consists of two fragments, one angular chunk and one edge fragment, which combine to form an edge piece that fractured laterally during its removal. The spatial data for one of these pieces is not available and as such it is impossible to identify the horizontal and vertical conjoining distance (Table 4).

The dorsal surface of this detachment preserves at least one previous removal from the side of the original hammerstone, indicating the repeated fragmentation of this stone along its edges and margins. The result was an increasingly rounded edge as the non-invasive edge fragments were detached. Refit Set 11, however, also records the second main fragmentation sequence at P100. In that sequence a

hammerstone exhibits significant volume loss through the 'slicing' of the edge of the hammerstone, with both the active plane and opposite surface detached at once, following initial minor edge fragmentation.

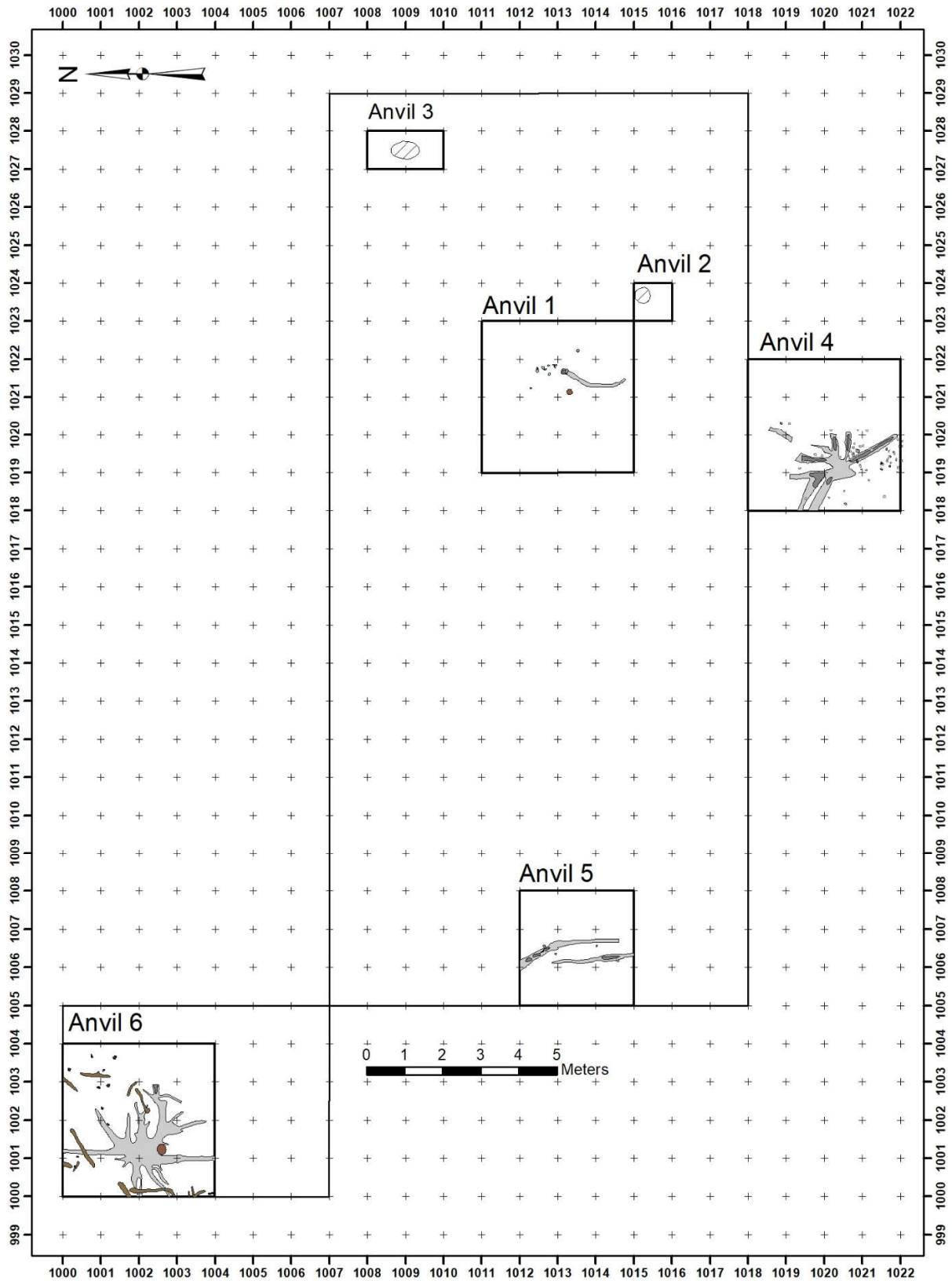
Refit Set 12

Refit Set 12 (Figure 8) includes five fragmented pieces, consisting of two edge fragments (Group 1.1), and three angular chunks / fragments (Groups 2.2 and 4). Although highly fragmented all pieces are derived from anvil 1 and represent a horizontal conjoining distance of 1.49m between three spits (Table 4). The refit retains evidence of two active percussive surfaces, bearing impact marks. Two pieces retain percussion marks in the form of localised crushing, which in one case resulted in the detachment of an edge fragment with an associated second removal of an internal angular chunk. In the second instance the percussive damage is located on the cortical surface of plane C, and is characterised as crushing that did not directly result in breakage of the hammerstone. For three of the five refitted fragments there is no clear association with percussive force, however, these fragments do possess clearly non-cortical surfaces suggesting an indirect fragmentation associated with percussive force. The detachment of these fragments can be explained by the poor quality, fractured, coarse grained and non-homogenous raw material.

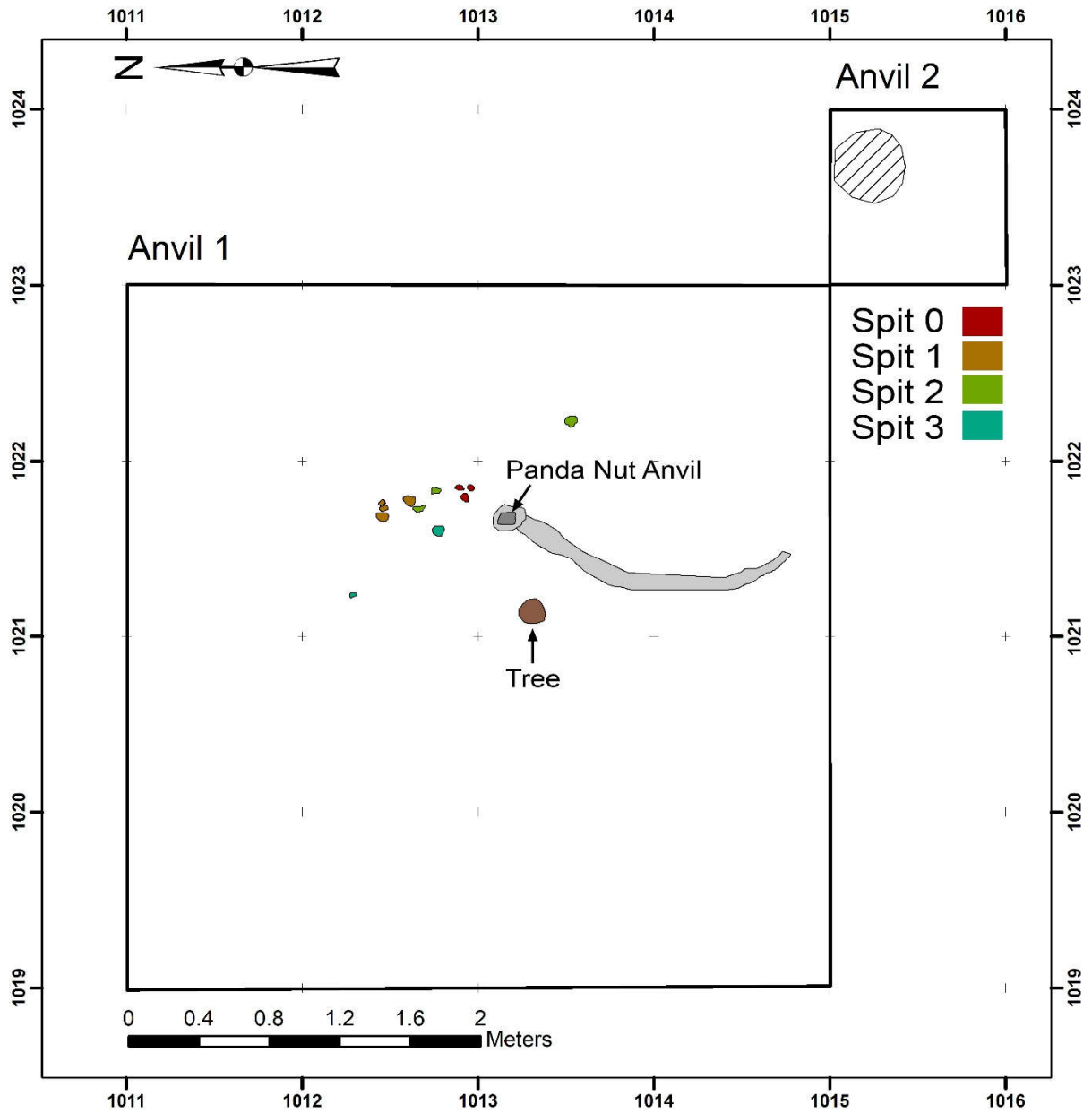
Similar to other refit sets, this refit represents the gradual attrition of the edge and exterior regions of a nut cracking hammerstone. This process is seen in the detachment of both small and large angular edge and corner fragments, gradually reducing the overall volume of the hammerstone.

Supplementary Material 3: GIS Maps

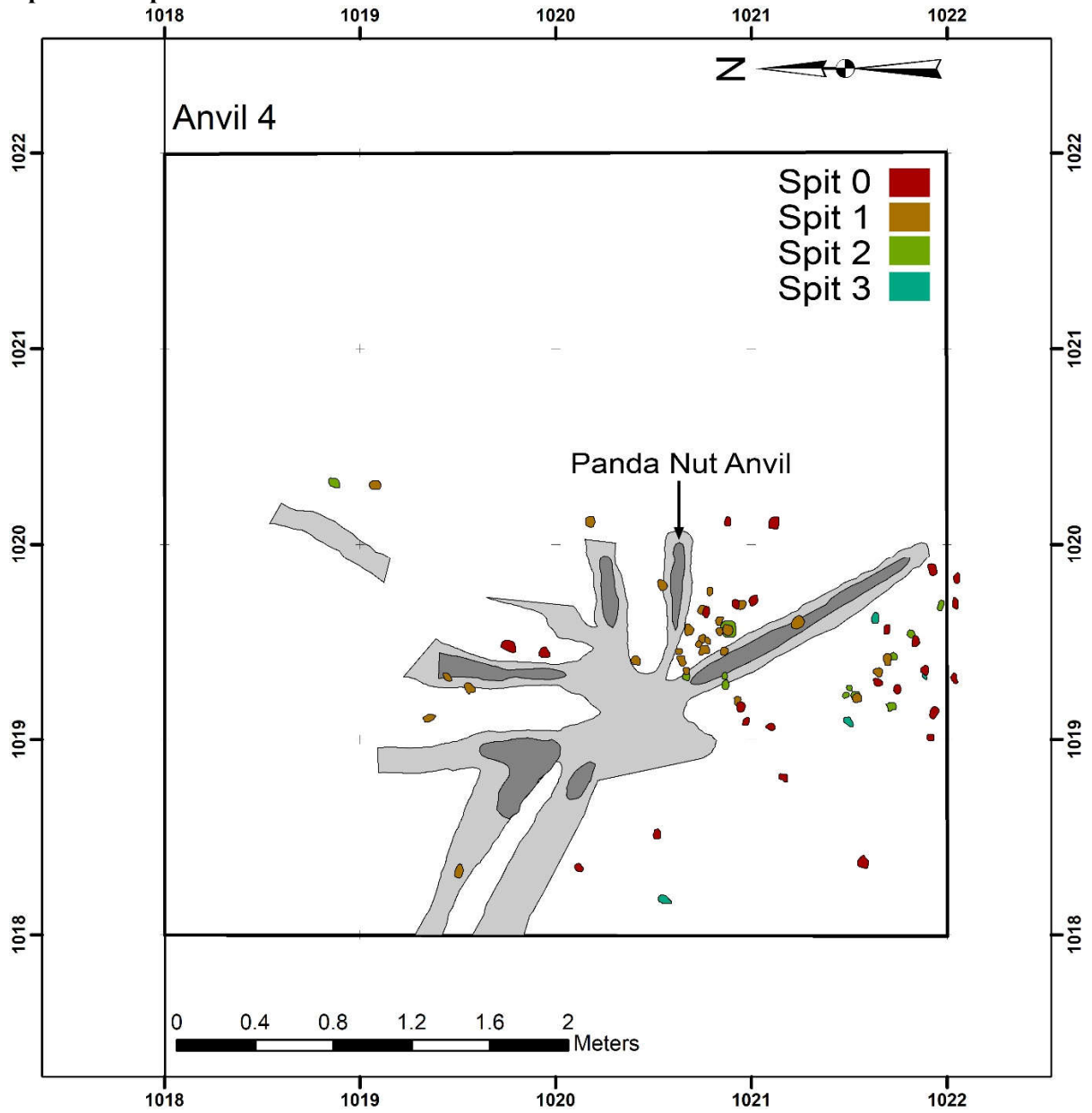
Map of Panda 100 excavation



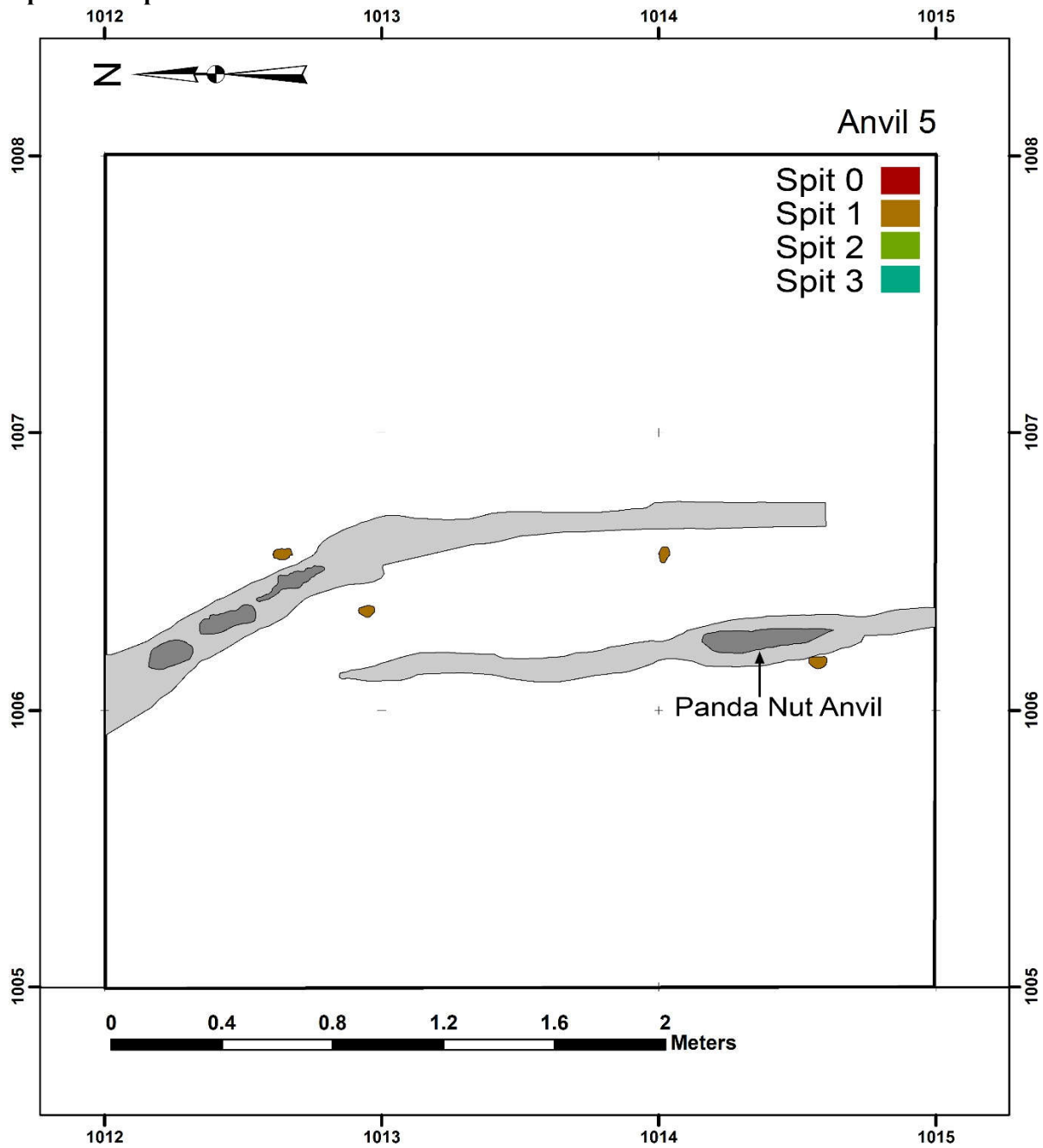
Updated Map of Panda 100 Anvil 1



Updated Map of Panda 100 Anvil 4



Updated Map of Panda 100 Anvil 5



Updated Map of Panda 100 Anvil 6

